This article has been accepted for publication in a future issue of this journal, but has not been fully edited. Content may change prior to final publication.
Citation information: DOI: 10.1109/TAC.2025.3627100, IEEE Transactions on Automatic Control

Zonotopic Polynomial Set-Membership Fusion Estimation for Nonlinear Systems via Carleman Approximation: An Encoding-Decoding Scheme

Zhongyi Zhao, Zidong Wang, Jinling Liang, and Wenying Xu

***Abstract*—In this paper, the zonotopic set-membership estimation (SME) problem is addressed for a class of nonlinear systems subjected to an encoding-decoding scheme, where the measurement information of each sensor is encoded and then transmitted to the remote fusion center. The objective of this paper is to develop a zonotope-based weighted measurement fusion method to fuse the received decoding signals, and to design a zonotopic SME algorithm that fully utilizes the higher-order partial derivatives of the nonlinear functions based on the fused signal. A zonotope-based weighted measurement fusion (WMF) method is proposed by means of the full rank decomposition technique, which enables the fusion of the decoding signals by solving a weighted least squares problem. To design the desired SME algorithm, the nonlinear system is first transformed into a linear time-varying system using the Carleman approximation technique. Then, based on the fused signal, a Kalman-type estimator is constructed and the zonotopes encompassing the prediction error and the estimation error are recursively calculated. The estimator parameter is obtained by minimizing the F-radius of the zonotope enclosing the estimation error at each time instant. Furthermore, effect of the system smoothness level on the F-radius is intensively analyzed. It is shown that incorporating the higher-order partial derivatives into the design of the SME algorithm enables the extraction of additional state constraints, and that the number of extractable constraints increases monotonically with the smoothness level. A method is subsequently proposed to leverage these constraints in order to improve the estimation accuracy. Moreover, the WMF method is proven to provide an equivalent estimation accuracy as compared to the most commonly used parallel fusion method while possessing lower computational complexity. Finally, two simulation experiments are conducted to demonstrate the efficacy and utility of the SME method.**

***Index Terms*—Zonotopic set-membership estimation, nonlinear systems, encoding-decoding scheme, Carleman approximation, weighted measurement fusion.**

This work was supported in part by the National Natural Science Foundation of China under Grants 62373103, 62403130, and 62573121; in part by the Jiangsu Provincial Scientific Research Center of Applied Mathematics of China under Grant BK20233002; in part by the Natural Science Foundation of Jiangsu Province of China under Grant BK20241286; in part by the Jiangsu Funding Program for Excellent Postdoctoral Talent of China under Grant 2024ZB601; in part by the China Postdoctoral Science Foundation-CCTEG Joint Support Program under Grant 2025T055ZGMK; in part by the Royal Society of the UK; and in part by the Alexander von Humboldt Foundation of Germany. (*Corresponding author: Jinling Liang*)

Zhongyi Zhao, Jinling Liang, and Wenying Xu are with the School of Mathematics, Southeast University, Nanjing 210096, China. (Emails: zhongyizhao@seu.edu.cn, jinlliang@seu.edu.cn, wyxu@seu.edu.cn)

Zidong Wang is with the Department of Computer Science, Brunel University London, Uxbridge, Middlesex, UB8 3PH, United Kingdom. (Email: Zidong.Wang@brunel.ac.uk)

I. Introduction

For several decades, set-membership estimation (SME) has been recognized as an effective technique for addressing state estimation problems in systems subjected to unknown-but-bounded (UBB) noises [19], [32], [38], [54]. This technique aims to calculate compact sets that enclose the actual system states at each moment in a recursive manner, based on the knowledge of the sets enclosing the initial system state and the external noises. As a typical class of compact sets, zonotopes have increasingly been applied in the field of SME, and numerous research contributions on zonotopic SME have been published in the literature, see e.g., [17], [46], [47], [49] and the references therein. This popularity is mainly due to the properties of zonotopes in set operations (including linear mapping and the Minkowski sum) and order reduction, which provide significant convenience to SME [16], [24], [39], [52].

Nonlinearities are widely acknowledged to be present in the majority of practical systems. Consequently, substantial research effort has been directed towards studying the SME of nonlinear systems, and a number of related results have been made available in the existing literature. For example, in [1], [45], the zonotopic SME problem has been investigated for nonlinear systems, where the zonotopes constraining the system states have been recursively calculated by means of the mean-value theorem. In [9], [41], the first-order Taylor expansion has been applied to the SME of nonlinear systems. It should be noted that, in almost all results concerning the SME of general nonlinear systems, the design of SME algorithms is based on the knowledge of the Jacobian matrix or the Hessian matrix of the nonlinear function, while the knowledge of the higher-order partial derivatives of the nonlinear functions has not been sufficiently utilized. It is worth noting that the Carleman approximation technique for nonlinear systems can fully utilize the knowledge of these higher-order partial derivatives, thereby improving estimation accuracy [10], [36], [37], [43]. As such, it is practically sensible to introduce the Carleman approximation technique into the zonotopic SME problem.

In recent years, network-based communications have played an increasingly important role in a wide range of industrial systems [15], [27], [33]. As a fundamental technique within network-based communications, the encoding-decoding scheme has attracted considerable research attention due to its unique ability to address network-induced issues, and many studies have reported on control and estimation problems under this mechanism [18], [34]. For instance, in [51], the consensus

tracking problem has been addressed for nonlinear discrete-time multi-agent systems, where a uniform-quantization-based encoding-decoding scheme is adopted to mitigate the effects of limited bandwidth. In [28], the resilient state estimation problem based on encoding-decoding has been studied for bias-corrupted stochastic nonlinear systems. Additionally, in [55], the distributed state estimation problem has been investigated for microgrids using encoding-decoding schemes. However, the effects of the encoding-decoding scheme on the zonotopic SME problem for nonlinear systems have not yet been fully explored, especially concerning the zonotopic SME problem under the Carleman-approximation-based polynomial estimation framework.

Fusion estimation has proven to be an effective state estimation technique for multi-sensor systems [7], [12], [13], [44], [50]. By properly processing measurements from multiple sensors, this technique can provide more accurate estimates of system states compared to single-sensor-based estimation [8], [53], [56]. Fusion estimation techniques are mainly categorized into two types: centralized fusion and distributed fusion [22], [31]. The primary difference between these two methods lies in whether raw measurements are directly employed. As a typical centralized fusion estimation method, the weighted measurement fusion (WMF) method, also known as data compression fusion, aims to form a compressed measurement with low dimension by weighting the system measurements. Using the compressed measurement in the design of estimation algorithms can significantly reduce computational costs [21], [23], [30]. Furthermore, it has been demonstrated that the same estimation accuracy could be achieved by employing the compressed measurement as compared to the parallel fusion method (i.e., one of the most commonly used centralized fusion methods that processes the measurements from multiple sensors by augmenting them into a single vector), provided that the weights of the measurements are properly designed [35]. Consequently, it is a natural progression to apply the WMF method to process the measurement information of the considered nonlinear system subjected to the encoding-decoding scheme.

Given the aforementioned analysis, the objective of this paper is to address the zonotopic polynomial SME problem for nonlinear systems with an encoding-decoding scheme through a measurement fusion approach. To tackle this problem, three primary challenges have been identified as follows.

1) How to fuse the signals received by the fusion center to obtain a weighted signal when the measurement information from multiple sensors is affected by UBB noises and the encoding-decoding mechanism?
2) How to formulate the high-order approximation error that arises from the use of the Carleman linearization technique in approximating the nonlinear function under the influence of UBB noises?
3) How to design the zonotopic set-membership estimator based on the fused signal in the presence of high-order approximation error?

In response to the identified challenges, the main contributions of this paper are summarized as follows.

1) To the best of the authors' knowledge, the Carleman approximation technique is, for the first time, applied to the SME problem of nonlinear systems with the aim of improving estimation accuracy. Furthermore, a new expression for the Carleman approximation error is presented, which is more convenient to handle within the SME framework.
2) The encoding-decoding scheme is introduced into the studied SME problem, making the obtained results more general and applicable to scenarios with limited network bandwidth.
3) A zonotope-based WMF method is presented to fuse the decoding signals, which can produce a compressed signal with a lower dimension, potentially reducing the computational burden associated with the Carleman approximation technique. Unlike the WMF methods in [23], [35], the proposed WMF method employs a new zonotope-based fusion criterion specifically designed to handle the signals corrupted by bounded noises.
4) A zonotopic polynomial SME algorithm is designed based on the fused signal, which follows a recursive structure, making it well-suited for online applications. The influence of the smoothness parameter ν, which stems from the assumption that the nonlinear system is $\nu+1$ times continuously differentiable, is analyzed in the context of the proposed algorithm. It is revealed that higher values of ν facilitate the extraction of additional constraint on the system state by leveraging the estimated Kronecker powers of the system state, and that the number of extractable constraints monotonically increases as ν does. Moreover, in order to enhance the estimation accuracy, a method is also presented to exploit these constraints.
5) It is proven that, under the established zonotope-based polynomial SME framework, the WMF method achieves the same estimation accuracy as the parallel fusion method, thereby extending a key result from the Kalman-filtering-based fusion theory to this new context.

Notations: $\mathbb{R}^n$ and $\mathbb{R}^{m\times n}$ denote the n-dimensional Euclidean space and the set of all $m\times n$ matrices, respectively. $\mathbb{N}$ denotes the set of natural numbers. $\mathrm{Tr}\{\cdot\}$ denotes the trace of a square matrix "$\cdot$". For sets D_1 and D_2, their Minkowski sum is defined as $D_1\oplus D_2 \triangleq \{d_1+d_2 : d_1\in D_1,\ d_2\in D_2\}$. For $M\in\mathbb{R}^{m\times n}$ and $D\subset\mathbb{R}^n$, the set $M\odot D$ is defined as $\{Md : d\in D\}$. I denotes an identity matrix of proper dimension. For matrices $A^{(1)},\dots,A^{(n)}$, $\mathrm{vec}_n\{A^{(\Im)}\}\triangleq[(A^{(1)})^T\ \cdots\ (A^{(n)})^T]^T$, and $\mathrm{diag}_n\{A^{(\Im)}\}\triangleq\mathrm{diag}\{A^{(1)},\dots,A^{(n)}\}$. For a matrix Z, $\|Z\|_\infty$ denotes its infinity norm. Given a matrix Z and a positive definite matrix P, $\|Z\|_P^2\triangleq Z^TPZ$. For a matrix Z with n rows, $\mathrm{rs}\{Z\}$ denotes the diagonal matrix $\mathrm{diag}_n\{\|Z_i\|_\infty\}$ with Z_i being the i-th row of Z.

II. Preliminaries

A. Zonotopes

Zonotopes will be used to constrain the external noises and provide bounds on the system states. The definition of a zonotope is provided as follows.

Definition 1: [26] An m-order zonotope with center $d \in \mathbb{R}^n$ and generator matrix $D \in \mathbb{R}^{n\times m}$, denoted as $\langle d, D\rangle \subset \mathbb{R}^n$, is defined as $\langle d, D\rangle \triangleq \{d + Dz : z \in \mathbb{R}^m, \|z\|_\infty \leq 1\}$.

The size of a zonotope can be characterized by its F-radius.

Definition 2: [14] The F-radius of a given zonotope $\langle d, D\rangle$ is defined as $\|D\|_F \triangleq \sqrt{\mathrm{Tr}\{DD^T\}}$.

The following are some properties of zonotopes.

Lemma 1: [24] For zonotopes $\langle d_1, D_1\rangle, \langle d_2, D_2\rangle \subset \mathbb{R}^n$ and a matrix $Z \in \mathbb{R}^{m\times n}$, the following properties hold:

$$\langle d_1, D_1\rangle \oplus \langle d_2, D_2\rangle = \langle d_1 + d_2, \begin{bmatrix} D_1 & D_2\end{bmatrix}\rangle$$
$$Z \odot \langle d_1, D_1\rangle = \langle Zd_1, ZD_1\rangle.$$

Lemma 2: [57] If a vector ϖ satisfies $\|\varpi\|_\infty \leq \bar{\varpi}$ where $\bar{\varpi}$ is a positive scalar, then the following relationship holds:

$$\varpi \in \langle 0, \bar{\varpi} I\rangle .$$

B. Kronecker Powers of Matrices

In this subsection, the definition of the Kronecker power of matrices will first be provided. In addition, the definition of Kronecker powers of the gradient operator applied to vector-valued functions will also be introduced. Both of these definitions will be utilized in the design of the SME algorithm based on the Carleman approximation.

Definition 3: [5] The Kronecker power of a matrix $D \in \mathbb{R}^{n\times m}$ is defined as

$$D^{[0]} = 1, \quad D^{[l]} = D^{[l-1]} \otimes D, \quad l = 1, 2, \ldots$$

where "$\otimes$" denotes the matrix Kronecker product.

Definition 4: [20] The operation $\nabla_x^{[i]}\otimes$ applied to a vector-valued function $f(x) : \mathbb{R}^n \mapsto \mathbb{R}^n$ is defined as

$$\nabla_x^{[0]} \otimes f = f$$
$$\nabla_x^{[l+1]} \otimes f = \nabla_x \otimes \nabla_x^{[l]} \otimes f, \quad l = 0, 1, 2, \ldots$$

with $\nabla_x \triangleq [\partial/\partial x^{(1)} \ \partial/\partial x^{(2)} \ \cdots \ \partial/\partial x^{(n)}]$. Here, $x^{(1)}$, $x^{(2)}$, ..., $x^{(n)}$ are the components of vector x, that is, $x = [x^{(1)} \ x^{(2)} \ \cdots \ x^{(n)}]^T$.

III. Problem Formulation

A. System Model

Consider the following nonlinear system:

$$x(k+1) = f(x(k), k) + w(k) \tag{1}$$

where $x(k) \in \mathbb{R}^n$ is the system state, $f(\cdot,\cdot) : \mathbb{R}^n \times \mathbb{N} \mapsto \mathbb{R}^n$ is a $\nu+1$ times continuously differentiable nonlinear function, and $w(k)$ is the UBB process noise. To facilitate the readers, all variables used in this paper are explained in Table I.

The system in (1) is measured by N sensors. The observation of the j-th sensor is described as follows:

$$y_j(k) = C_j(k)x(k) + v_j(k), \quad j = 1, 2, \ldots, N$$

where $y_j(k) \in \mathbb{R}^{m_j}$ is the measurement output, $v_j(k)$ is the UBB measurement noise, and $C_j(k)$ is the measurement matrix.

Assumption 1: The noises $w(k)$, $v_j(k)$ $(j \in \{1, 2, \ldots, N\})$ and the initial state $x(0)$ satisfy

$$w(k) \in \langle 0, \mathrm{diag}_n\{\mathbf{w}^{(i)}\}\rangle \triangleq \langle 0, \mathbf{W}\rangle$$

TABLE I: Variable list

Variable	Meaning
$x(k), \hat{x}(k)$	System state and its estimate
$\tilde{x}(k)$	State of the augmented system
$\widehat{x}(k\|k-1), \widehat{x}(k\|k)$	One-step prediction and estimation of $\tilde{x}(k)$
$\vec{\mathbf{X}}(0)$	Parameter of the zonotope containing $x(0)$
$\mathbf{x}(l,0), \mathbf{X}(l,0)$	Parameters of the zonotope containing $x^{[l]}(0)$
$\tilde{\mathbf{x}}(0), \tilde{\mathbf{X}}(0)$	Parameters of the zonotope containing $\tilde{x}(0)$
$y_j(k), \breve{y}_j(k)$	Outputs of the j-th sensor and the j-th decoder
$\breve{y}(k), \acute{y}(k)$	Signals before and after compression
$w(k)$	Process noise
$\mathbf{W}$	Parameter of the zonotope containing $w(k)$
$\mathbf{w}(l), \mathbf{W}(l)$	Parameters of the zonotope containing $w^{[l]}(k)$
$\vec{w}(l,k)$	Equivalent process noise in $x^{[l+1]}(k+1)$
$\tilde{\mathbf{w}}(l,k)I_{n^l}$	Parameter of the zonotope containing $\vec{w}(l,k)$
$\tilde{w}(k)$	Equivalent process noise in $\tilde{x}(k+1)$
$\tilde{\mathbf{W}}(k)$	Parameter of the zonotope containing $\tilde{w}(k)$
$v_j(k)$	Measurement noise in the j-th sensor
$\mathbf{V}_j$	Parameter of the zonotope containing $v_j(k)$
$\breve{v}_j(k)$	Equivalent noise in the decoding signal $\breve{y}_j(k)$
$\breve{\mathbf{V}}_j$	Parameter of the zonotope containing $\breve{v}_j(k)$
$\breve{v}(k)$	Equivalent noise in the decoding signal $\breve{y}(k)$
$\breve{\mathbf{V}}$	Parameter of the zonotope containing $\breve{v}(k)$
$\acute{v}(k)$	Equivalent noise in the compressed signal $\acute{y}(k)$
$\acute{\mathbf{V}}(k)$	Parameter of the zonotope containing $\acute{v}(k)$
$\vec{\mathscr{O}}(l,k), \mathscr{O}(k)$	Remainders in $x^{[l]}(k+1)$ and $\tilde{x}(k+1)$
$\overleftarrow{\mathscr{O}}(l,k)$	Parameter of the zonotope containing $\vec{\mathscr{O}}(l,k)$
$\tilde{\mathscr{O}}(k)$	Parameter of the zonotope containing $\mathscr{O}(k)$
$C_j(k)$	Measurement matrix of the j-th sensor
$C(k)$	Measurement matrix of the system
$H(k), \mathcal{M}(k)$	The factors of a full rank decomposition for $C(k)$
$\mathcal{Q}(k)$	Weight matrix in the WLS estimation problem
$\mathcal{K}(k)$	Estimator gain matrix
$K(k)$	Parameter to be designed in $\mathcal{K}(k)$
$\underline{\mathcal{E}}(k)$	Parameter of the zonotope containing $e(k\|k-1)$
$\mathcal{E}(k)$	Parameter of the zonotope containing $e(k\|k)$

$$v_j(k) \in \left\langle 0, \mathrm{diag}_{m_j}\left\{\mathbf{v}_j^{(\sigma)}\right\}\right\rangle \triangleq \langle 0, \mathbf{V}_j\rangle$$
$$x(0) \in \langle 0, \mathrm{diag}_n\{\mathbf{x}^{(i)}(0)\}\rangle \triangleq \langle 0, \vec{\mathbf{X}}(0)\rangle$$

respectively. Here, $\mathbf{w}^{(i)}$, $\mathbf{x}^{(i)}(0)$ $(i = 1, 2, \ldots, n)$, and $\mathbf{v}_j^{(\sigma)}$ $(\sigma = 1, 2, \ldots, m_j)$ are known positive scalars.

Remark 1: In this paper, the nonlinear function $f(\cdot,\cdot)$ in system (1) is assumed to be known and $\nu+1$ times continuously differentiable. This assumption is commonly satisfied for those systems with mechanistic models. Typical examples include the systems modeled as discrete-time nonlinear systems (such as the prey-predator system [42] and the population growth model [2]) as well as the systems obtained by discretizing the continuous counterparts (such as those in power harmonic detection [4] and the mobile robots [3], [58]). For systems subject to model uncertainties or unmodeled dynamics, this assumption can still hold as long as the uncertainties are reasonably bounded [59]. Note that such an assumption has also been explicitly/implicitly made in the SME issue of nonlinear systems, see e.g., [6], [11].

For most practical systems, the knowledge on their noises and the initial states is often limited to certain conservative bounds. In such a case, the interval vectors (a special type of zonotopes with diagonal generator matrices, as described in [24]) just represent the tightest set bounding these uncertainties, which infers the rationale behind Assumption 1 and explains why it has been widely adopted in SME studies [14], [52]. Note that, in engineering applications, the parameters $\mathbf{W}$ and $\mathbf{V}_j$ $(j = 1, 2, \ldots, N)$ must be chosen large enough to ensure that Assumption 1 holds. Otherwise, performance of the SME may not be guaranteed. At the same time, these parameters should be set to make the interval vectors in Assumption 1 as tight as possible, in order to reduce conservatism and improve estimation performance. For this purpose, a realistic way to set these parameters is to use prior knowledge such as physical system constraints or measurement accuracy. Another way is to adopt the empirical data such as the observed noise magnitudes.

B. Encoding-Decoding Scheme

To reduce the network transmission burden, the dynamic-quantization-based encoding-decoding scheme proposed in [29] is employed for the measurement of each sensor in this paper. The main principle of this mechanism is described as follows.

For $j = 1, 2, \ldots, N$, the signal $y_j(k)$ is *first* encoded according to the following rule:

$$\begin{cases} \zeta_j(0) = 0 \\ o_j(k) = Q_j\Big(\dfrac{1}{\varsigma_j}(y_j(k) - \zeta_j(k-1))\Big) \\ \zeta_j(k) = \varsigma_j o_j(k) + \zeta_j(k-1) \end{cases} \tag{2}$$

where $\zeta_j(k)$ and $o_j(k)$ are the internal state and the generated codeword of the encoder, respectively; ς_j is a pre-set positive scalar; and, for vector $z = [z^{(1)}\ z^{(2)}\ \cdots\ z^{(m_j)}]^T \in \mathbb{R}^{m_j}$, $Q_j(z)$ is the quantizer described as follows:

$$Q_j(z) = \begin{bmatrix} \mathfrak{Q}_j(z^{(1)}) & \mathfrak{Q}_j(z^{(2)}) & \cdots & \mathfrak{Q}_j(z^{(m_j)}) \end{bmatrix}^T. \tag{3}$$

Here, for $\sigma = 1, 2, \ldots, m_j$, if $(2\chi - 1)\tau_j/2 \le z^{(\sigma)} < (2\chi + 1)\tau_j/2$, function $\mathfrak{Q}_j(z^{(\sigma)})$ is defined as

$$\mathfrak{Q}_j(z^{(\sigma)}) \triangleq \chi\tau_j \tag{4}$$

where τ_j is a given positive scalar and $\chi = 0, \pm 1, \pm 2, \ldots$. The codeword $o_j(k)$ is *then* sent to the decoder, in which $o_j(k)$ is reconstructed according to the following decoding rule:

$$\begin{cases} \breve{y}_j(0) = 0 \\ \breve{y}_j(k) = \varsigma_j o_j(k) + \breve{y}_j(k-1) \end{cases} \tag{5}$$

where $\breve{y}_j(k)$ denotes the output of the decoder.

Define $\Delta_j(k) \triangleq \frac{1}{\varsigma_j}(y_j(k) - \zeta_j(k-1)) - o_j(k)$ and $\breve{v}_j(k) \triangleq v_j(k) - \varsigma_j\Delta_j(k)$. With (2)–(5), the output of the decoder $\breve{y}_j(k)$ can be rewritten as

$$\breve{y}_j(k) = C_j(k)x(k) + \breve{v}_j(k) \tag{6}$$

where the signal $\breve{v}_j(k)$ satisfies

$$\breve{v}_j(k) \in \Big\langle 0, \operatorname{diag}\big\{\breve{\mathbf{v}}_j^{(1)}, \breve{\mathbf{v}}_j^{(2)}, \ldots, \breve{\mathbf{v}}_j^{(m_j)}\big\}\Big\rangle \triangleq \langle 0, \breve{\mathbf{V}}_j\rangle \tag{7}$$

with $\breve{\mathbf{v}}_j^{(\sigma)} \triangleq \mathbf{v}_j^{(\sigma)} + \varsigma_j\tau_j/2$ for $\sigma = 1, 2, \ldots, m_j$.

Remark 2: To facilitate the sequel analysis and synthesis, a zonotope enclosing the additive signal $\breve{v}_j(k)$, which consists of the measurement noise $v_j(k)$ and the coding error $-\varsigma_j\Delta_j(k)$, is derived in (7) by using Definition 1 and Lemma 1. The method handling the coding error described above is also applicable to the processing of other bounded/additive signals in system measurements within the polynomial SME framework. Note that, under the influence of random disturbances, the existing polynomial estimation methods face difficulties in handling the additive signals in the measurement data [37].

C. Problem Statement

The aim of this paper is to achieve the following three objectives.

1) Establish a zonotope-based measurement fusion method to fuse the decoding signals $\breve{y}_j(k)$ $(j = 1, 2, \ldots, N)$.
2) Design an SME algorithm based on the fused decoding signal that can utilize the knowledge of the higher-order partial derivatives of the nonlinear function $f(\cdot)$ (i.e., $\nabla_x^{[q]} \otimes f(\cdot)$ with $q = 2, 3, \ldots$) to recursively calculate the zonotopes enclosing the system state $x(k)$.
3) Compare the estimation accuracy of the WMF method and the parallel fusion method under the established zonotope-based polynomial SME framework.

IV. Main Results

We begin by presenting a zonotope-based WMF method that fuses the decoded signals.

A. Zonotope-Based WMF Method

To process the decoding signals $\breve{y}_j(k)$ $(j = 1, 2, \ldots, N)$, let

$$\breve{y}(k) \triangleq \begin{bmatrix} \breve{y}_1^T(k) & \breve{y}_2^T(k) & \cdots & \breve{y}_N^T(k) \end{bmatrix}^T.$$

Then, one has from (6) that

$$\breve{y}(k) = C(k)x(k) + \breve{v}(k) \tag{8}$$

where $C(k) = \operatorname{vec}_N\{C_j(k)\}$, $\breve{v}(k) = \operatorname{vec}_N\{\breve{v}_j(k)\}$.

By means of the full rank decomposition technique, one obtains

$$C(k) = H(k)\mathcal{M}(k) \tag{9}$$

where $H(k)$ is a full-column-rank matrix and $\mathcal{M}(k)$ is a full-row-rank matrix.

Based on (8) and (9), one derives the weighted least square (WLS) estimation of $\mathcal{M}(k)x(k)$ as follows:

$$\acute{y}(k) = \arg\min_{\breve{y}^*(k)} \|\breve{y}(k) - H(k)\breve{y}^*(k)\|^2_{\mathcal{Q}(k)}$$

where $\acute{y}(k) \in \mathbb{R}^{\acute{r}(k)}$ is the desired WLS estimation of $\mathcal{M}(k)x(k)$ with $\acute{r}(k) = \operatorname{rank}(C(k))$, and $\mathcal{Q}(k)$ is a given positive definite matrix.

From [60], $\acute{y}(k)$ can be expressed as

$$\acute{y}(k) = \big(H^T(k)\mathcal{Q}(k)H(k)\big)^{-1} H^T(k)\mathcal{Q}(k)\breve{y}(k). \tag{10}$$

Then, substituting (8) into (10), one has

$$\acute{y}(k) = \mathcal{M}(k)x(k) + \acute{v}(k) \tag{11}$$

where

$$\acute{v}(k) = \left(H^T(k)\mathcal{Q}(k)H(k)\right)^{-1} H^T(k)\mathcal{Q}(k)\breve{v}(k). \tag{12}$$

In accordance with (7), it is easy to derive from Definition 1 that

$$\breve{v}(k) \in \langle 0, \mathrm{diag}_N\{\breve{\mathbf{V}}_j\}\rangle \triangleq \langle 0, \breve{\mathbf{V}}\rangle \tag{13}$$

which, together with (12), further indicates that

$$\begin{aligned}\acute{v}(k) &\in \left\langle 0, \left(H^T(k)\mathcal{Q}(k)H(k)\right)^{-1} H^T(k)\mathcal{Q}(k)\breve{\mathbf{V}}\right\rangle \\ &\triangleq \langle 0, \acute{\mathbf{V}}(k)\rangle.\end{aligned} \tag{14}$$

From (14), it is clear that the size of the zonotope $\langle 0, \acute{\mathbf{V}}(k)\rangle$ can be optimized by appropriately selecting the matrix $\mathcal{Q}(k)$. In the following proposition, matrix $\mathcal{Q}(k)$ that can minimize the F-radius of the zonotope $\langle 0, \acute{\mathbf{V}}(k)\rangle$ will be given.

Proposition 1: Consider the case where the matrix $\mathcal{Q}(k)$ is to be designed. If $\mathcal{Q}(k)$ is selected as

$$\mathcal{Q}(k) = \left(\breve{\mathbf{V}}\breve{\mathbf{V}}^T\right)^{-1} \tag{15}$$

then the F-radius of the zonotope $\langle 0, \acute{\mathbf{V}}(k)\rangle$ in (14) is minimized.

Proof: The proof of this proposition is similar to that of the well-known batch WLS estimation (see e.g., [25], [30]) and is therefore omitted here. ∎

In the rest of this paper, matrix $\mathcal{Q}(k)$ is set to be $(\breve{\mathbf{V}}\breve{\mathbf{V}}^T)^{-1}$ to minimize the F-radius of the zonotope enclosing signal $\acute{v}(k)$.

B. Polynomial Nonlinear Systems

To fully utilize the information contained in the higher-order partial derivatives of the nonlinear function $f(\cdot)$, a polynomial nonlinear system will be derived in this subsection. For this purpose, it is necessary to deduce the zonotopes constraining the Kronecker powers of the process noise $w(k)$. To achieve this, a lemma (i.e., Lemma 4) is proposed in Appendix A.

With $w(k) \in \langle 0, \mathbf{W}\rangle$ given in Assumption 1, one has

$$w^{[l]}(k) \in \langle \mathbf{w}(l), \mathbf{W}(l)\rangle, \quad l = 1, 2, \ldots, \nu \tag{16}$$

where $\mathbf{w}(l)$ and $\mathbf{W}(l)$ are obtained by using Lemma 4.

After deducing the zonotopes restraining the Kronecker powers of the process noise $w(k)$, in the following, the polynomial nonlinear system will be given based on the Carleman approximation technique.

By means of the Taylor polynomial around a given point $\hat{x}(k)$, the l-th Kronecker power of the nonlinear system in (1) can be expressed as

$$\begin{aligned}x^{[l]}(k+1) = &\sum_{h=0}^{\nu} \mathscr{F}(l, h, \hat{x}(k), w(k), k)(x(k) - \hat{x}(k))^{[h]} \\ &+ \vec{\mathscr{O}}(l, k)\end{aligned} \tag{17}$$

where

$$\mathscr{F}(l, h, \hat{x}(k), w(k), k) = \frac{1}{h!}\left(\nabla_x^{[h]} \otimes (f + w)^{[l]}\right)\Big|_{x(k)=\hat{x}(k)}$$

$$\vec{\mathscr{O}}(l, k) = \mathscr{R}(l, \breve{x}(k), w(k), k)(x(k) - \hat{x}(k))^{[\nu+1]}$$

$$\begin{aligned}\mathscr{R}(l, \breve{x}(k), w(k), k) = &\frac{1}{(\nu+1)!} \\ &\cdot \mathrm{vec}_{n^l}\left\{\left(\nabla_x^{[\nu+1]} \otimes \left(\Lambda^{(\Im)}(f + w)^{[l]}\right)\right)\Big|_{x(k)=\Gamma^{(\Im)}\breve{x}(k)}\right\}\end{aligned}$$

$$\Lambda^{(\Im)} = [\underbrace{0 \ \cdots \ 0}_{\Im-1} \ \ 1 \ \ \underbrace{0 \ \cdots \ 0}_{n^l-\Im}]$$

$$\Gamma^{(\Im)} = \Lambda^{(\Im)} \otimes I_n$$

$$\breve{x}(k) = \Theta(k) \otimes x(k) + (\mathbf{1}_{n^l} - \Theta(k)) \otimes \hat{x}(k)$$

$$\mathbf{1}_{n^l} = [\underbrace{1 \ \ 1 \ \ \cdots \ \ 1}_{n^l}]^T$$

$$\Theta(k) = \mathrm{vec}_{n^l}\left\{\theta^{(\Im)}(k)\right\}$$

with $\theta^{(1)}(k)$, $\theta^{(2)}(k)$, …, $\theta^{(n^l)}(k) \in [0, 1]$.

Remark 3: Unlike the results in [36], [37], where the Carleman approximation error is formulated to improve the estimation accuracy, in this paper, the Carleman approximation error (i.e., $\vec{\mathscr{O}}(l, k)$) must be considered to ensure the SME performance. To address this, a new expression of the approximation error is proposed in (17). Note that such an expression differs from those in [36], [37] and is more convenient to handle within the zonotopic SME framework.

To derive the desired polynomial nonlinear system, the following lemma will be needed.

Lemma 3: [10] For any integer $l \geq 0$ and vectors $a, b \in \mathbb{R}^n$, one has

$$(a + b)^{[l]} = \sum_{h=0}^{l} M(l, h, n)\left(a^{[h]} \otimes b^{[l-h]}\right)$$

where $M(l, h, n)$ $(h = 0, 1, \ldots, l)$ are suitably defined matrices.

With the center $\mathbf{w}(l)$ of the zonotope in (16), for a given estimate $\hat{x}(k)$ of $x(k)$, it can be obtained from (17) and Lemma 3 that

$$x^{[l]}(k+1) = \sum_{q=0}^{\nu} \vec{\mathscr{A}}(l, q, k)x^{[q]}(k) + \vec{w}(l, k) + \vec{\mathscr{O}}(l, k) \tag{18}$$

where

$$\begin{aligned}&\vec{\mathscr{A}}(l, q, k) \\ &= \sum_{p=0}^{l}\sum_{h=q}^{\nu} \frac{1}{h!} M(l, p, n)\Big(\left(\left(\nabla_x^{[h]} \otimes f^{[p]}\right)\Big|_{x(k)=\hat{x}(k)}\right) \\ &\quad \otimes \mathbf{w}(l-p)\Big) M(h, q, n)\left(I_{n^q} \otimes (-\hat{x}(k))^{[h-q]}\right)\end{aligned} \tag{19}$$

$$\begin{aligned}&\vec{w}(l, k) \\ &= \sum_{h=0}^{\nu}\sum_{p=0}^{l} \frac{1}{h!} M(l, p, n)\Big\{\Big(\left(\left(\nabla_x^{[h]} \otimes f^{[p]}\right)\Big|_{x(k)=\hat{x}(k)}\right) \\ &\quad \cdot (x(k) - \hat{x}(k))^{[h]}\Big) \otimes \left(w^{[l-p]} - \mathbf{w}(l-p)\right)\Big\}\end{aligned} \tag{20}$$

and $\mathbf{w}(0) = 1$.

Define

$$\tilde{x}(k) \triangleq \left[1 \quad x^T(k) \quad \left(x^{[2]}(k)\right)^T \quad \cdots \quad \left(x^{[\nu]}(k)\right)^T\right]^T.$$

Then, one has from (18) that

$$\tilde{x}(k+1) = \mathscr{A}(k)\tilde{x}(k) + \tilde{w}(k) + \mathscr{O}(k) \tag{21}$$

where

$$\mathscr{A}(k) = \begin{bmatrix} \vec{\mathscr{A}}(0,0,k) & \vec{\mathscr{A}}(0,1,k) & \cdots & \vec{\mathscr{A}}(0,\nu,k) \\ \vec{\mathscr{A}}(1,0,k) & \vec{\mathscr{A}}(1,1,k) & \cdots & \vec{\mathscr{A}}(1,\nu,k) \\ \vdots & \vdots & \ddots & \vdots \\ \vec{\mathscr{A}}(\nu,0,k) & \vec{\mathscr{A}}(\nu,1,k) & \cdots & \vec{\mathscr{A}}(\nu,\nu,k) \end{bmatrix}$$

$$\tilde{w}(k) = \begin{bmatrix} \vec{w}^T(0,k) & \vec{w}^T(1,k) & \cdots & \vec{w}^T(\nu,k) \end{bmatrix}^T$$

$$\mathscr{O}(k) = \begin{bmatrix} \vec{\mathscr{O}}^T(0,k) & \vec{\mathscr{O}}^T(1,k) & \cdots & \vec{\mathscr{O}}^T(\nu,k) \end{bmatrix}^T.$$

With $x(0) \in \langle 0, \vec{\mathbf{X}}(0) \rangle$ given in Assumption 1, one can obtain

$$x^{[l]}(0) \in \langle \mathbf{x}(l,0), \mathbf{X}(l,0) \rangle, \quad l = 1, 2, \ldots, \nu \tag{22}$$

where $\mathbf{x}(l,0)$ and $\mathbf{X}(l,0)$ are calculated by Lemma 4. Based on (22), it is easy to see that the initial value of the augmented system (21) satisfies

$$\tilde{x}(0) \in \left\langle \tilde{\mathbf{x}}(0), \tilde{\mathbf{X}}(0) \right\rangle \tag{23}$$

where

$$\tilde{\mathbf{x}}(0) = \begin{bmatrix} 1 & (\mathrm{vec}_\nu\{\mathbf{x}(l,0)\})^T \end{bmatrix}^T$$
$$\tilde{\mathbf{X}}(0) = \mathrm{diag}\big\{0, \mathrm{diag}_\nu\{\mathbf{X}(l,0)\}\big\}.$$

To estimate the state of the system in (21) by using the fused signal $\acute{y}(k)$ in (11), one needs to further transform it based on the augmented state $\tilde{x}(k)$. It can be deduced that

$$\acute{y}(k) = \acute{\mathcal{M}}(k)\tilde{x}(k) + \acute{v}(k) \tag{24}$$

where $\acute{\mathcal{M}}(k) = \mathcal{M}(k)\mathcal{I}$ with

$$\mathcal{I} = \begin{bmatrix} 0_{n\times 1} & I_n & 0_{n\times n^2} & \cdots & 0_{n\times n^\nu} \end{bmatrix}.$$

Remark 4: So far, the desired polynomial nonlinear system has been derived as in (21) and (24). To achieve this, it can be observed from (18)–(20) that the zonotope enclosing $w^{[l]}(k)$ (see (16)) plays a crucial role. This zonotope is obtained using Lemma 4 under the assumption that the generator matrix $\mathbf{W}$ of the zonotope containing $w(k)$ is diagonal (see Assumption 1). In fact, such a diagonal assumption is not strictly necessary when deriving the zonotope enclosing $w^{[l]}(k)$. If $\mathbf{W}$ is not diagonal, Lemma 4 can still be applied by just over-approximating the zonotope $\langle 0, \mathbf{W} \rangle$ with another larger zonotope $\langle 0, \mathrm{rs}\{\mathbf{W}\} \rangle$, where $\mathrm{rs}\{\mathbf{W}\}$ is obviously a diagonal matrix.

C. Estimator Design

Construct the following estimator for the system in (21):

$$\widehat{x}(k+1|k) = \mathscr{A}(k)\widehat{x}(k|k) \tag{25}$$

$$\widehat{x}(k+1|k+1) = \widehat{x}(k+1|k) + \mathcal{K}(k+1)\big(\acute{y}(k+1) - \acute{\mathcal{M}}(k+1)\widehat{x}(k+1|k)\big) \tag{26}$$

$$\widehat{x}(0|0) = \tilde{\mathbf{x}}(0) \tag{27}$$

where $\widehat{x}(k+1|k)$ is the prediction of $\tilde{x}(k+1)$, $\widehat{x}(k+1|k+1)$ is the estimate of $\tilde{x}(k+1)$, and $\mathcal{K}(k+1)$ has the form of

$$\mathcal{K}(k+1) = \begin{bmatrix} 0_{\acute{r}(k+1)\times 1} & K^T(k+1) \end{bmatrix}^T \tag{28}$$

with $K(k+1)$ being the estimator gain matrix to be designed.

Define $e(k|k-1) \triangleq \tilde{x}(k) - \widehat{x}(k|k-1)$ and $e(k|k) \triangleq \tilde{x}(k) - \widehat{x}(k|k)$. It follows from (21), (24), (25) and (26) that

$$e(k+1|k) = \mathscr{A}(k)e(k|k) + \tilde{w}(k) + \mathscr{O}(k) \tag{29}$$

$$e(k+1|k+1) = \big(I - \mathcal{K}(k+1)\acute{\mathcal{M}}(k+1)\big)e(k+1|k) - \mathcal{K}(k+1)\acute{v}(k+1). \tag{30}$$

Furthermore, it is easily seen from (23) and (27) that

$$e(0|0) \in \left\langle 0, \tilde{\mathbf{X}}(0) \right\rangle. \tag{31}$$

In the following theorem, based on the assumption that the estimation error $e(k|k)$ belongs to a zonotope, an approach is proposed to calculate the zonotope enclosing $e(k+1|k+1)$.

Theorem 1: Let the estimate $\widehat{x}(k|k)$ be given. Suppose that the estimation error $e(k|k)$ in (30) satisfies

$$e(k|k) \in \langle 0_{\bar{n}\times 1}, \mathcal{E}(k) \rangle. \tag{32}$$

Then, the prediction error $e(k+1|k)$ and the estimation error $e(k+1|k+1)$ satisfy

$$e(k+1|k) \in \left\langle 0_{\bar{n}\times 1}, \begin{bmatrix} \mathscr{A}(k)\mathcal{E}(k) & \tilde{\mathbf{W}}(k) & \tilde{\mathscr{O}}(k) \end{bmatrix} \right\rangle \triangleq \langle 0_{\bar{n}\times 1}, \underline{\mathcal{E}}(k+1) \rangle \tag{33}$$

$$e(k+1|k+1) \in \Big\langle 0_{\bar{n}\times 1}, \big[(I - \mathcal{K}(k+1)\acute{\mathcal{M}}(k+1))\underline{\mathcal{E}}(k+1) - \mathcal{K}(k+1)\acute{\mathbf{V}}(k+1)\big] \Big\rangle \triangleq \langle 0_{\bar{n}\times 1}, \mathcal{E}(k+1) \rangle \tag{34}$$

where $\bar{n} \triangleq (1 - n^{\nu+1})/(1-n)$, and

$$\tilde{\mathbf{W}}(k) \triangleq \mathrm{diag}\left\{\tilde{\mathbf{w}}(0,k), \tilde{\mathbf{w}}(1,k)I_n, \ldots, \tilde{\mathbf{w}}(\nu,k)I_{n^\nu}\right\} \tag{35}$$

$$\tilde{\mathbf{w}}(l,k) \triangleq \begin{cases} 0, & l = 0 \\ \displaystyle\sum_{h=0}^{\nu}\sum_{p=0}^{l} \frac{1}{h!}\|M(l,p,n)\|_\infty \cdot \|\mathcal{E}_1(k)\|_\infty^h \\ \qquad \cdot \|(\nabla_x^{[h]} \otimes f^{[p]})|_{x(k)=\hat{x}(k)}\|_\infty \\ \qquad \cdot \|\mathbf{W}(l-p)\|_\infty, & l = 1, \ldots, \nu \end{cases} \tag{36}$$

$$\mathbf{W}(0) \triangleq 0, \qquad \hat{x}(k) \triangleq \mathcal{I}\widehat{x}(k|k), \qquad \mathcal{E}_1(k) \triangleq \mathcal{I}\mathcal{E}(k) \tag{37}$$

$$\tilde{\mathscr{O}}(k) \triangleq \mathrm{diag}\big\{\overleftarrow{\mathscr{O}}(0,k), \overleftarrow{\mathscr{O}}(1,k), \ldots, \overleftarrow{\mathscr{O}}(\nu,k)\big\} \tag{38}$$

$$\overleftarrow{\mathscr{O}}(l,k) \triangleq \tilde{o}(l,k)I_{n^l}, \quad l = 0, 1, \ldots, \nu \tag{39}$$

$$\tilde{o}(l,k) \triangleq \frac{1}{(\nu+1)!}\|\mathcal{E}_1(k)\|_\infty^{\nu+1} \cdot \sum_{p=0}^{l} F(p,k) \cdot \|M(l,p,n)\|_\infty \cdot (\|\mathbf{w}(l-p)\|_\infty + \|\mathbf{W}(l-p)\|_\infty) \tag{40}$$

$$F(p,k) \triangleq \max_{x(k)\in\langle \hat{x}(k), \mathcal{E}_1(k)\rangle} \big\|\nabla_x^{[\nu+1]} \otimes f^{[p]}\big\|_\infty. \tag{41}$$

Proof: Please see Appendix C. ∎

Theorem 2: Assume that the estimator parameter $K(k+1)$ is designed as

$$K(k+1) = \mathscr{I}^T\underline{\mathcal{P}}(k+1)\acute{\mathcal{M}}^T(k+1)\Phi^{-1}(k+1) \tag{42}$$

where

$$\begin{aligned}
&\mathscr{I} \triangleq \begin{bmatrix} 0_{(\bar{n}-1)\times 1} & I_{\bar{n}-1} \end{bmatrix}^T \\
&\underline{\mathcal{P}}(k+1) \triangleq \underline{\mathcal{E}}(k+1)\underline{\mathcal{E}}^T(k+1) \\
&\Phi(k+1) \triangleq \acute{\mathcal{M}}(k+1)\underline{\mathcal{P}}(k+1)\acute{\mathcal{M}}^T(k+1) \\
&\qquad\qquad + \acute{\mathbf{V}}(k+1)\acute{\mathbf{V}}^T(k+1).
\end{aligned}$$

Then, the F-radius of the zonotope in (34) is minimized.

Proof: Please see Appendix D. ∎

Remark 5: In Theorem 2, it has been proven that the F-radius of the zonotope restraining the estimation error of the augmented system (21) is minimized when the parameter $K(k+1)$ is given by (42). With the calculated parameter $K(k+1)$ and the initial condition (31), one can recursively calculate the zonotopes containing $e(k+1|k)$ and $e(k+1|k+1)$ by using the induction and the results of Theorem 1. Notably, the higher-order partial derivatives of the nonlinear function $f(\cdot)$ are fully utilized in deriving such a zonotope.

In many instances, one may be more interested in the size of the zonotope enclosing the estimation error of the original state $x(k)$. Based on the relationship between $x(k)$ and $\tilde{x}(k)$ (i.e., $x(k) = \mathcal{I}\tilde{x}(k)$), the zonotope containing the system state $x(k)$ can be expressed by

$$\begin{aligned}
x(k) &= \mathcal{I}\widehat{x}(k|k) + \mathcal{I}e(k|k) \\
&\in \mathcal{I}\widehat{x}(k|k) \oplus (\mathcal{I} \odot \langle 0_{\bar{n}\times 1}, \mathcal{E}(k)\rangle) \\
&= \langle \mathcal{I}\widehat{x}(k|k), \mathcal{I}\mathcal{E}(k)\rangle = \langle \hat{x}(k), \mathcal{E}_1(k)\rangle. \qquad (43)
\end{aligned}$$

For the F-radius of the zonotope in (43), we have the following proposition.

Proposition 2: Suppose that the estimator parameter $K(k)$ is designed by (42). Then, the F-radius of zonotope $\langle \hat{x}(k), \mathcal{E}_1(k)\rangle$ is minimized.

Proof: Please see Appendix E. ∎

As a summary of the derived results, an SME algorithm (i.e., Algorithm 1) is proposed.

Remark 6: The computational complexity of Algorithm 1 mainly depends on the dimension n of the system state, the dimension $\acute{r}(k)$ of the compressed signal, and the order ν of the Taylor expansion. Let $\aleph$ be the number of floating-point operations (FLOPs) required to compute $(\nabla_x^{[\nu]} \otimes f^{[\nu]})|_{x(k)=\hat{x}(k)}$ and $\bar{m} \triangleq \sum_{j=1}^{N} m_j$. The FLOPs for some key computational steps of Algorithm 1 are given in Table II. From the table, the following observations can be made: 1) Apart from $\tilde{\mathscr{O}}(k-1)$, the $O(n^{3\nu} + n^{2\nu}\mathcal{N})$ terms dominate the overall computational complexity of Algorithm 1. 2) The FLOPs for computing $\tilde{\mathscr{O}}(k-1)$ largely depend on the complexity of the algorithm used to solve the optimization problem in (41). 3) As ν increases, the computational complexity of Algorithm 1 grows exponentially.

D. Improvement of the Estimation Performance When $\nu \geq 2$

As discussed in the above subsection, the established polynomial SME algorithm (i.e., Algorithm 1) uses the higher-order partial derivatives of the nonlinear function with orders from 1 to ν. Intuitively, a larger ν is expected to enhance the estimation performance more, provided that the considered nonlinear system has continuous partial derivatives up to the

Algorithm 1: The SME algorithm

Input: Scalar ν and matrices $\mathbf{W}$, $\mathbf{V}_j$ $(j = 1, 2, \ldots, N)$, $\vec{\mathbf{X}}(0)$.
Output: $\widehat{x}(k|k)$ and $\mathcal{E}(k)$.

Initialization:
Compute $\check{\mathbf{V}}_j$ by (7);
Compute $\check{\mathbf{V}}$ by (13);
Compute $\langle \mathbf{w}(l), \mathbf{W}(l)\rangle$ in (16) and $\langle \mathbf{x}(l,0), \mathbf{X}(l,0)\rangle$ in (22) for $l = 1, 2, \cdots, \nu$ by Lemma 4;
Give the maximum simulation time $k_{\max}$ and a positive integer $\mathcal{N}$;
Compute $\widehat{x}(0|0)$ by (27);
Set $k = 0$ and $\mathcal{E}(0) = \tilde{\mathbf{X}}(0)$;
for $k = 1 : k_{\max}$ **do**
  Compute $\hat{x}(k-1)$ by (37);
  Compute $\mathscr{A}(k-1)$ according to (19);
  Update $\widehat{x}(k|k-1)$ by (25) ;
  Compute $\tilde{\mathbf{W}}(k-1)$ by (35) and (36);
  Compute $\tilde{\mathscr{O}}(k-1)$ by (38)–(41);
  Compute $\underline{\mathcal{E}}(k)$ by (33);
  Compute $\mathcal{Q}(k)$ by (15);
  Obtain $H(k)$ and $\mathcal{M}(k)$ by (9);
  Obtain $\acute{y}(k)$ by (8) and (10);
  Compute $\acute{\mathcal{M}}(k)$ by (9) and $\acute{\mathcal{M}}(k) = \mathcal{M}(k)\mathcal{I}$;
  Compute $\acute{\mathbf{V}}(k)$ by (14);
  Compute $K(k)$ by (42);
  Compute $\widehat{x}(k|k)$ by (26);
  Compute $\mathcal{E}(k)$ by (34);
  if *the number of columns of* $\mathcal{E}(k)$ *is greater than* $\mathcal{N}$ **then**
    set $\mathcal{E}(k) = \mathrm{rs}\{\mathcal{E}(k)\}$;
  Output $\widehat{x}(k|k)$ and $\mathcal{E}(k)$;

TABLE II: FLOPs of the primary computational steps in Algorithm 1.

Steps of Algorithm 1	FLOP counts
$\mathscr{A}(k-1)$	$O\left(n^{3\nu}\right)$
$\widehat{x}(k\|k-1)$	$O\left(n^{2\nu}\right)$
$\tilde{\mathbf{W}}(k-1)$	$O(n^{2\nu}\aleph + n\mathcal{N})$
$\tilde{\mathscr{O}}(k-1)$	depending on $F(\nu, k-1)$
$\underline{\mathcal{E}}(k)$	$O(n^{2\nu}\mathcal{N})$
$\mathcal{Q}(k)$	$O(\bar{m}^2)$
$H(k)$ and $\mathcal{M}(k)$	$O((\max(n, \bar{m}))^3)$
$\acute{y}(k)$	$O(\bar{m}^2\acute{r}(k))$
$\acute{\mathbf{V}}(k)$	$O(\bar{m}^2\acute{r}(k))$
$K(k)$	$O(n^{2\nu}\acute{r}(k) + n^{\nu}\acute{r}^2(k))$
$\widehat{x}(k\|k)$	$O(n^{\nu}\acute{r}(k))$
$\mathcal{E}(k)$	$O(n^{2\nu}\mathcal{N})$

corresponding order. However, as illustrated in Example 2 of Section V, increasing ν does not necessarily reduce the F-radius of the zonotope bounding the system state (i.e., $\|\mathcal{E}_1(k)\|_F$). Nevertheless, a higher value of ν does provide additional information about the system state $x(k)$, enabling more accurate correction of the state estimation in (43). Specifically, from the definition of $e(k|k)$, Theorem 1 and Definition 1, there must exist a vector $\eta(k)$ with $\|\eta(k)\|_\infty \leq 1$ such that $\tilde{x}(k) = \widehat{x}(k|k) + \mathcal{E}(k)\eta(k)$, which further leads to

$$\tilde{x}^{[2:\nu]}(k) = \widehat{x}^{[2:\nu]}(k|k) + \mathcal{E}^{[2:\nu]}(k)\eta(k) \tag{44}$$

where $\tilde{x}^{[2:\nu]}(k)$ denotes the vector by removing the first $1+n$ entries from $\tilde{x}(k)$ (i.e., $\tilde{x}^{[2:\nu]}(k) \triangleq [(x^{[2]}(k))^T \quad (x^{[3]}(k))^T \quad \cdots \quad (x^{[\nu]}(k))^T]^T$); $\widehat{x}^{[2:\nu]}(k|k)$ denotes the corresponding sub-vector of $\widehat{x}(k|k)$, which is also the estimate for $\tilde{x}^{[2:\nu]}(k)$; and $\mathcal{E}^{[2:\nu]}(k)$ denotes the corresponding sub-matrix of $\mathcal{E}(k)$. Equation (44) imposes additional constraint on the system state $x(k)$, namely

$$x(k) \in \Re \triangleq \{x(k) : \tilde{x}^{[2:\nu]}(k) - \widehat{x}^{[2:\nu]}(k|k) \in \langle 0, \mathcal{E}^{[2:\nu]}(k)\rangle\}$$

which, together with (43), yields

$$x(k) \in \Re \cap \langle \hat{x}(k), \mathcal{E}_1(k)\rangle. \tag{45}$$

This indicates that the state estimation of $x(k)$ can be further refined through additional constraint (44). Note that a larger value of ν will introduce more constraints on $x(k)$, because the dimension of $\widehat{x}^{[2:\nu]}(k|k)$ increases with respect to ν.

Although the above discussions highlight the advantages of the proposed method in improving the estimation accuracy when $\nu \geq 2$, calculating a zonotope that tightly bounds the intersection presented in (45) is generally cumbersome and computationally inefficient. To address this issue, we will propose an alternative method that facilitates the incorporation of the constraint given in (44) in a computationally tractable manner.

Note that equality (44) can be interpreted as a nonlinear measurement equation for the system state $x(k)$, where $\widehat{x}^{[2:\nu]}(k|k)$ serves as the measurement output, $\tilde{x}^{[2:\nu]}(k)$ is a nonlinear function of $x(k)$, and $-\mathcal{E}^{[2:\nu]}(k)\eta(k)$ acts as the measurement noise belonging to the zonotope $\langle 0, \mathcal{E}^{[2:\nu]}(k)\rangle$. In order to utilize this nonlinear measurement equation for correcting the estimation $\hat{x}(k)$ in (43), applying the Taylor polynomial around $\hat{x}(k)$ to $\tilde{x}^{[2:\nu]}(k)$ yields

$$\tilde{x}^{[2:\nu]}(k) = \sum_{h=0}^{\nu} \Xi_h(k)(x(k) - \hat{x}(k))^{[h]} \tag{46}$$

where $\Xi_h(k) = \frac{1}{h!}(\nabla_x^{[h]} \otimes \tilde{x}^{[2:\nu]})|_{x(k)=\hat{x}(k)}$. Based on (44) and (46), we construct a corrected estimate, denoted as $\underline{\hat{x}}(k)$, as follows:

$$\underline{\hat{x}}(k) = \hat{x}(k) + L(k)\big(\widehat{x}^{[2:\nu]}(k|k) - \tilde{x}^{[2:\nu]}(k)|_{x(k)=\hat{x}(k)}\big) \tag{47}$$

where $L(k)$ is the estimator gain to be designed. Let $\underline{\hat{e}}(k) \triangleq x(k) - \underline{\hat{x}}(k)$ be the corresponding estimation error. Then, combing (43) and (47), we obtain

$$\underline{\hat{e}}(k) = (I - L(k)\Xi_1(k))\mathcal{I}e(k|k) + L(k)\mathcal{E}^{[2:\nu]}(k)\eta(k)$$
$$- L(k)\sum_{h=2}^{\nu} \Xi_h(k)(x(k) - \hat{x}(k))^{[h]}. \tag{48}$$

In the following theorem, the zonotope bounding $\underline{\hat{e}}(k)$ and the estimator gain $L(k)$ that can minimize the F-radius of such a zonotope will be given.

Theorem 3: The estimation error $\underline{\hat{e}}(k)$ satisfies

$$\begin{aligned}\underline{\hat{e}}(k) \in \big\langle 0, [(I - L(k)\Xi_1(k))\mathcal{E}_1(k) \quad -\kappa(k)L(k) \\ L(k)\mathcal{E}^{[2:\nu]}(k)]\big\rangle \\ \triangleq \langle 0, \underline{\hat{\mathcal{E}}}_1(k)\rangle\end{aligned} \tag{49}$$

where

$$\kappa(k) = \sum_{h=2}^{\nu} \frac{1}{h!}\left\|\left(\nabla_x^{[h]} \otimes \tilde{x}^{[2:\nu]}\right)\Big|_{x(k)=\hat{x}(k)}\right\|_\infty \cdot \|\mathcal{E}_1(k)\|_\infty^h.$$

Moreover, if $L(k)$ is designed as

$$\begin{aligned}L(k) =& \mathcal{E}_1(k)\mathcal{E}_1^T(k)\Xi_1^T(k)\big(\Xi_1(k)\mathcal{E}_1(k)\mathcal{E}_1^T(k)\Xi_1^T(k) \\ &+ \kappa^2(k)I + \mathcal{E}^{[2:\nu]}(k)(\mathcal{E}^{[2:\nu]}(k))^T\big)^{-1}\end{aligned} \tag{50}$$

then $\|\underline{\hat{\mathcal{E}}}_1(k)\|_F$ is minimized as

$$\begin{aligned}\|\underline{\hat{\mathcal{E}}}_1(k)\|_F^2 = \|\mathcal{E}_1(k)\|_F^2 - \mathrm{Tr}\big\{&\mathcal{E}_1(k)\mathcal{E}_1^T(k)\Xi_1^T(k) \\ &\cdot \big(\Xi_1(k)\mathcal{E}_1(k)\mathcal{E}_1^T(k)\Xi_1^T(k) + \kappa^2(k)I + \mathcal{E}^{[2:\nu]}(k) \\ &\cdot (\mathcal{E}^{[2:\nu]}(k))^T\big)^{-1}\Xi_1(k)\mathcal{E}_1(k)\mathcal{E}_1^T(k)\big\}.\end{aligned} \tag{51}$$

Proof: Please see Appendix F. ■

Remark 7: The above discussions imply that, when $\nu \geq 2$, estimating the term $\tilde{x}^{[2:\nu]}(k)$ would introduce an extra constraint on the system state $x(k)$, as shown in (44) and (45). Such a constraint enables refinement of the estimation obtained from Algorithm 1 and (43), thereby further improving the estimation accuracy. Theorem 3 just provides a detailed technique that exploits this constraint to enhance the estimation accuracy, where improvement of the estimation accuracy can be observed/declared from (51).

Recall that a larger ν not only introduces more constraint on the system state $x(k)$, enabling further correction of the estimation obtained by Algorithm 1 and (43), but also causes an exponential increase in the computational complexity. Therefore, in practical applications, ν should be appropriately selected to be as large as possible, provided that the resulting computational complexity remains within an acceptable range.

Remark 8: The polynomial SME method is developed in this paper based on the WMF method. It is well known that the WMF method can achieve a same estimation accuracy as that of the widely used parallel fusion estimation method, which acquires the state estimate using signals that are obtained by augmenting the measurement information from multiple sensors within the Kalman-filtering-based fusion framework [35]. One question naturally raises, i.e., whether a similar performance guarantee holds under the proposed polynomial SME framework? This question will be addressed in the next subsection.

E. Comparison Between the WMF Method and the Parallel Fusion Method Under the Established Polynomial SME Framework

In this subsection, the proposed WMF method will be compared with the parallel fusion method within the established zonotope-based polynomial SME framework. To facilitate this comparison, the results of the polynomial set-membership estimator under the parallel fusion scheme are provided as follows.

Under the parallel fusion scheme, the measurement equation (8) for system (21) can be rewritten as

$$\breve{y}(k) = C(k)\mathcal{I}\tilde{x}(k) + \breve{v}(k). \tag{52}$$

Based on (52), construct the following estimator for the system (21):

$$\widehat{x}^{\mathrm{PF}}(k+1|k) = \mathscr{A}(k)\widehat{x}^{\mathrm{PF}}(k|k) \tag{53}$$

$$\begin{aligned}\widehat{x}^{\mathrm{PF}}(k+1|k+1) = \widehat{x}^{\mathrm{PF}}(k+1|k) + \mathcal{K}^{\mathrm{PF}}(k+1)\big(\breve{y}(k+1) \\ - C(k+1)\mathcal{I}\widehat{x}^{\mathrm{PF}}(k+1|k)\big)\end{aligned} \tag{54}$$

$$\widehat{x}^{\mathrm{PF}}(0|0) = \tilde{\mathbf{x}}(0)$$

where the superscript "PF" represents that the estimator is constructed under the parallel fusion scheme, $\widehat{x}^{\mathrm{PF}}(k+1|k)$ is the prediction of $\tilde{x}(k+1)$, $\widehat{x}^{\mathrm{PF}}(k+1|k+1)$ is the estimate of $\tilde{x}(k+1)$, and $\mathcal{K}^{\mathrm{PF}}(k+1)$ is in the form of

$$\mathcal{K}^{\mathrm{PF}}(k+1) = \begin{bmatrix} 0_{\bar{m}\times 1} & (K^{\mathrm{PF}}(k+1))^T \end{bmatrix}^T \tag{55}$$

with $K^{\mathrm{PF}}(k+1)$ being the estimator parameter.

Let the estimate $\widehat{x}^{\mathrm{PF}}(k|k)$ be given, and assume that the estimation error $e^{\mathrm{PF}}(k|k) \triangleq \tilde{x}(k) - \widehat{x}^{\mathrm{PF}}(k|k)$ satisfies

$$e^{\mathrm{PF}}(k|k) \in \langle 0_{\bar{n}\times 1}, \mathcal{E}^{\mathrm{PF}}(k)\rangle.$$

Then, on the basis of the developed theorems on the WMF estimator, it is easy to obtain that the prediction error $e^{\mathrm{PF}}(k+1|k) \triangleq \tilde{x}(k+1) - \widehat{x}^{\mathrm{PF}}(k+1|k)$ and the estimation error $e^{\mathrm{PF}}(k+1|k+1)$ satisfy

$$\begin{aligned} e^{\mathrm{PF}}(k+1|k) &\in \left\langle 0_{\bar{n}\times 1}, \begin{bmatrix} \mathscr{A}(k)\mathcal{E}^{\mathrm{PF}}(k) & \tilde{\mathbf{W}}^{\mathrm{PF}}(k) & \tilde{\mathscr{O}}^{\mathrm{PF}}(k) \end{bmatrix} \right\rangle \\ &\triangleq \langle 0_{\bar{n}\times 1}, \underline{\mathcal{E}}^{\mathrm{PF}}(k+1)\rangle \end{aligned} \tag{56}$$

$$\begin{aligned} e^{\mathrm{PF}}(k+1|k+1) &\in \Big\langle 0_{\bar{n}\times 1}, \Big[\big(I - \mathcal{K}^{\mathrm{PF}}(k+1)C(k+1)\mathcal{I}\big) \\ &\quad \times \underline{\mathcal{E}}^{\mathrm{PF}}(k+1) \quad -\mathcal{K}^{\mathrm{PF}}(k+1)\breve{\mathbf{V}} \Big] \Big\rangle \\ &\triangleq \langle 0_{\bar{n}\times 1}, \mathcal{E}^{\mathrm{PF}}(k+1)\rangle \end{aligned} \tag{57}$$

where the expressions of $\tilde{\mathbf{W}}^{\mathrm{PF}}(k)$ and $\tilde{\mathscr{O}}^{\mathrm{PF}}(k)$ are similar to $\tilde{\mathbf{W}}(k)$ and $\tilde{\mathscr{O}}(k)$ in Theorem 1 and thus omitted here for saving space. Moreover, it can be seen that, if parameter $K^{\mathrm{PF}}(k+1)$ is designed as

$$K^{\mathrm{PF}}(k+1) = \mathscr{I}^T\underline{\mathcal{P}}^{\mathrm{PF}}(k+1)\mathcal{I}^T C^T(k+1)(\Phi^{\mathrm{PF}}(k+1))^{-1} \tag{58}$$

where

$$\begin{aligned} \underline{\mathcal{P}}^{\mathrm{PF}}(k+1) &\triangleq \underline{\mathcal{E}}^{\mathrm{PF}}(k+1)(\underline{\mathcal{E}}^{\mathrm{PF}}(k+1))^T \\ \Phi^{\mathrm{PF}}(k+1) &\triangleq C(k+1)\mathcal{I}\underline{\mathcal{P}}(k+1)\mathcal{I}^T C^T(k+1) + \breve{\mathbf{V}}\breve{\mathbf{V}}^T \end{aligned}$$

then the F-radius of the zonotope in (57) is minimized.

In the following theorem, it is demonstrated that the WMF method and the parallel fusion method yield equivalent estimation accuracy under the established zonotope-based polynomial SME framework.

Theorem 4: Let the estimator parameters $K(k+1)$ and $K^{\mathrm{PF}}(k+1)$ be designed by (42) and (58), respectively. Assume that

$$\widehat{x}(k|k) = \widehat{x}^{\mathrm{PF}}(k|k) \tag{59}$$

$$\mathcal{E}(k) = \mathcal{E}^{\mathrm{PF}}(k). \tag{60}$$

Then, it follows that

$$\widehat{x}(k+1|k+1) = \widehat{x}^{\mathrm{PF}}(k+1|k+1) \tag{61}$$

$$\mathcal{E}(k+1) = \mathcal{E}^{\mathrm{PF}}(k+1). \tag{62}$$

Proof: Please see Appendix G. ∎

Remark 9: Under the parallel fusion scheme, it is noted that the method established in Subsection IV-D is also applicable to the polynomial SME. Let $\underline{\hat{x}}^{\mathrm{PF}}(k)$ and $\underline{\hat{\mathcal{E}}}_1^{\mathrm{PF}}(k)$ denote the counterparts of $\underline{\hat{x}}(k)$ and $\underline{\hat{\mathcal{E}}}_1(k)$, respectively, in the parallel fusion setting. Under the conditions of Theorem 4, it can be easily proved that $\underline{\hat{x}}^{\mathrm{PF}}(k) = \underline{\hat{x}}(k)$ and $\underline{\hat{\mathcal{E}}}_1^{\mathrm{PF}}(k) = \underline{\hat{\mathcal{E}}}_1(k)$.

Remark 10: By means of the full rank decomposition and the WLS techniques, the proposed zonotope-based WMF method produces a fused signal with lower dimensionality, thereby reducing the computational cost of the designed SME algorithm. To be specific, it can be seen that the WMF method and the parallel fusion method have the same complexity when calculating the one-step prediction and the zonotope enclosing the one-step prediction error, but when generating the estimation and the zonotope containing the estimation error, the required FLOPs for computing $K(k+1)$ and $K^{\mathrm{PF}}(k+1)$ are $\acute{r}^3(k) + (4\bar{n}+1)\acute{r}^2(k) + (2\bar{n}^2 - 3\bar{n} + 1)\acute{r}(k)$ (with given $\acute{\mathbf{V}}(k+1)\acute{\mathbf{V}}^T(k+1)$) and $\bar{m}^3 + (4\bar{n}+1)\bar{m}^2 + (2\bar{n}^2 - 3\bar{n} + 1)\bar{m}$ (with given $C(k+1)\mathcal{I}$ and $\breve{\mathbf{V}}\breve{\mathbf{V}}^T$), respectively. Furthermore, the proposed WMF method is shown to achieve equivalent estimation accuracy to that of the parallel fusion method under the established polynomial SME framework.

Remark 11: The proposed polynomial SME method for nonlinear systems requires an accurate model, as described in (1). In the situation where such a model is not available, data-driven SME methods might serve as an alternative. However, estimating the higher-order partial derivatives directly from the data remains a significant challenge. Addressing such an issue will be an important direction for the future researches.

V. Illustrative Examples

Example 1: In this example, we employ a permanent magnet synchronous motor (PMSM) modified from [40] to show the utility of Algorithm 1.

The dynamic equation of PMSM is given as follows:

$$\dot{i}_d = \frac{u_d - R_s i_d + p_n\omega_r L_q i_q}{L_d} + w^{(1)}$$

$$\dot{i}_q = \frac{u_q - R_s i_q - p_n\omega_r(L_d i_d + \psi_f)}{L_q} + w^{(2)}$$

$$\dot{\omega}_r = \frac{1.5p_n(\psi_f i_q + (L_d - L_q)i_d i_q) - T_L - \mu\omega_r}{J} + w^{(3)}$$

where i_d and i_q are the d axis and the q axis stator currents, ω_r is the rotor speed; u_d and u_q are the d axis and the q axis voltages, R_s is the stator resistance, L_d and L_q are respectively the d axis and the q axis inductances; p_n is the number of pole pairs, ψ_f is the flux linkage resulted from the rotor magnets linking the stator, T_L is the load torque, μ is the damping coefficient, J is the moment of inertia; and $w^{(i)}$ $(i = 1, 2, 3)$ describe the external disturbances.

By using the Euler discretization with sampling period $\bar{T}$, the discrete-time counterpart of PMSM can be obtained as follows:

$$\begin{aligned} i_d(k+1) &= \bar{T}\frac{u_d(k) - R_s i_d(k) + p_n\omega_r(k)L_q i_q(k)}{L_d} \\ &\quad + i_d(k) + \bar{T}w^{(1)}(k) \\ i_q(k+1) &= \bar{T}\frac{u_q(k) - R_s i_q(k) - p_n\omega_r(k)(L_d i_d(k) + \psi_f)}{L_q} \\ &\quad + i_q(k) + \bar{T}w^{(2)}(k) \\ \omega_r(k+1) &= \bar{T}\frac{1.5p_n(\psi_f i_q(k) + (L_d - L_q)i_d(k)i_q(k))}{J} \\ &\quad - \bar{T}\frac{T_L + \mu\omega_r(k)}{J} + \omega_r(k) + \bar{T}w^{(3)}(k). \end{aligned}$$

The measurements of PMSM are given as follows:

$$\begin{aligned} &y_1(k) = i_d(k) + v_1(k), \quad y_2(k) = i_d(k) + v_2(k) \\ &y_3(k) = i_q(k) + v_3(k). \end{aligned}$$

In this example, to better illustrate effectiveness of the proposed estimation method, the control input of PMSM is set to be $u_d(k) = 0\,\mathrm{V}$ and $u_q(k) = 50\,\mathrm{V}$, under which the PMSM becomes unstable. Other parameters are given by $\bar{T} = 0.1\,\mathrm{s}$, $R_s = 0.2\,\Omega$, $L_d = 0.01\,\mathrm{H}$, $L_q = 0.015\,\mathrm{H}$, $p_n = 4$, $\psi_f = 0.2\,\mathrm{Wb}$, $T_L = 2\,\mathrm{N}\cdot\mathrm{m}$, $\mu = 0.004\,\mathrm{N}\cdot\mathrm{m}\cdot\mathrm{s}\cdot\mathrm{rad}^{-1}$, and $J = 0.002\,\mathrm{kg}\cdot\mathrm{m}^2$. The initial state is set as $(i_d(0), i_q(0), \omega_r(0)) = (0.05, 0.1, 0.1)$. The noise terms $\bar{T}w^{(i)}(k)$ $(i = 1, 2, 3)$ and $v_j(k)$ $(j = 1, 2, 3)$ are all drawn from a uniform distribution on $[-0.1, 0.1]$. Corresponding, we set $\mathbf{W} = 0.1I$, $\mathbf{V}_j = 0.1$ $(j = 1, 2, 3)$, and $\vec{\mathbf{X}}(0) = 0.1I$. The encoders' parameters are given by $\varsigma_1 = \varsigma_2 = \varsigma_3 = 0.1$ and $\tau_1 = \tau_2 = \tau_3 = 0.05$.

Let $x(k) = [i_d(k) \quad i_q(k) \quad \omega_r(k)]^T$. Fig. 1 depicts the three state components of $x(k)$, along with their estimates and bounds. Their estimates and bounds are given by $\hat{x}(k) = \mathcal{I}\widehat{x}(k|k)$ and $\hat{x}(k) \pm \mathrm{rs}\{\mathcal{E}_1(k)\}\mathbf{1}$, respectively. To demonstrate advantages of the proposed method over the existing ones, it is compared with four representative methods: the SME method with state-dependent coefficient parameterization [6], the nonlinear estimation method using the second-order Taylor series expansion [11], the dual SME method [48], and the zonotopic SME method via semi-infinite programming [49]. Fig. 2 reports two metrics: 1) the F-radius of the zonotope restraining the actual state $x(k)$ (i.e., $\|\mathcal{E}_1(k)\|_F$) under different ν, and 2) the 2-norm of the estimation error (i.e., $\|x(k) - \hat{x}(k)\|_2$) across methods mentioned above. From this figure, it can be seen that 1) the proposed method achieves a smaller F-radius compared to the mean-value theorem based method in [1], and the performance under $\nu = 2$ is comparable to that under $\nu = 1$ in terms of $\|\mathcal{E}_1(k)\|_F$; and 2) the estimation error $\|x(k) - \hat{x}(k)\|_2$ under $\nu = 2$ is smaller than that under $\nu = 1$, where the average estimation errors computed over the first 10 time steps as $(1/10)\sum_{k=1}^{10}\|x(k) - \hat{x}(k)\|_2$ are derived respectively as 0.1869 and 0.2211. Moreover, the proposed method yields smaller estimation errors than the methods in [6], [11], [48], [49]. Note that all comparisons are conducted under the same external noises. These results further demonstrate effectiveness of the proposed method.

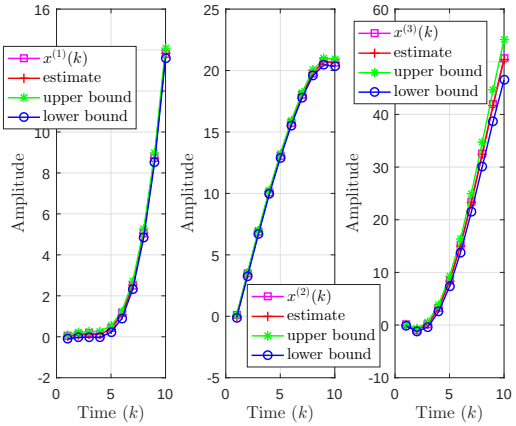

Fig. 1: Three components of the state variable, their estimates and bounds.

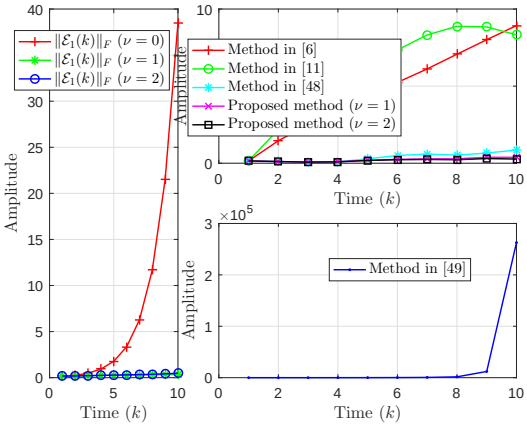

Fig. 2: Comparisons of $\|\mathcal{E}_1(k)\|_F$ under different ν (Left) and estimation errors $\|x(k) - \hat{x}(k)\|_2$ under different methods (Right).

Finally, to examine robustness of the proposed method, we further evaluate its performance under measurement noises obeying different distributions. Specifically, four scenarios are considered. In the $\imath$-th scenario ($\imath \in \{1, 2, 3, 4\}$), the measurement noise is given by $v(k) = [v_1(k) \quad v_2(k) \quad v_3(k)]^T$, where $v(k) = \vec{V}_\imath \vec{v}(k)$. Here, $\vec{V}_\imath$ $(\imath = 1, 2, 3, 4)$ are matrices describing the coupling strengths between the noise components which are taken as

$$\vec{V}_1 = \begin{bmatrix} 0.1 & 0.2 & 0 \\ 0 & 0.3 & 0.1 \\ 0.3 & 0.2 & 0 \end{bmatrix}, \quad \vec{V}_2 = \begin{bmatrix} 0.1 & 0 & 0.2 \\ 0.2 & 0.2 & 0 \\ 0 & 0.3 & 0.2 \end{bmatrix},$$
$$\vec{V}_3 = \begin{bmatrix} 0.3 & 0 & 0 \\ 0 & 0.4 & 0 \\ 0 & 0 & 0.5 \end{bmatrix}, \quad \vec{V}_4 = \begin{bmatrix} 0.1 & 0.1 & 0.1 \\ 0.2 & 0.1 & 0.1 \\ 0.2 & 0.2 & 0.1 \end{bmatrix}.$$

The symbol $\vec{v}(k) = [\vec{v}_1(k) \quad \vec{v}_2(k) \quad \vec{v}_3(k)]^T$ denotes a stochastic noise given as follows:

- Case 1: $\vec{v}_1(k)$, $\vec{v}_2(k)$, and $\vec{v}_3(k)$ are drawn from uniform distributions on $[0.1, 0.2]$, $[0.2, 0.3]$, and $[0.3, 0.5]$, respectively;
- Case 2: $\vec{v}_1(k)$, $\vec{v}_2(k)$, and $\vec{v}_3(k)$ are sampled from the standard normal distribution truncated to the intervals $[0.5, 0.7]$, $[0.7, 0.9]$, and $[0.9, 1]$, respectively;
- Case 3: $\vec{v}_1(k)$, $\vec{v}_2(k)$, and $\vec{v}_3(k)$ are independently sampled from the scaled Beta distributions. To be more specific, they are generated by $\vec{v}_1(k) = 0.5 + 0.2\flat(k)$, $\vec{v}_2(k) = 0.6+0.3\flat(k)$, and $\vec{v}_3(k) = 0.8+0.2\flat(k)$, respectively, where $\flat(k)$ obeys a Beta distribution $\mathrm{Beta}(2, 5)$ defined on interval $[0, 1]$;
- Case 4: for $\jmath = 1, 2, 3$, $\vec{v}_\jmath(k)$ follows the distribution specified in Case $\jmath$.

By taking $\mathbf{V}_1 = 0.3$, $\mathbf{V}_2 = 0.4$, and $\mathbf{V}_3 = 0.5$, it can be verified that Assumption 1 is always satisfied in the above four scenarios.

Under the setting of $\nu = 2$, Fig. 3 presents the average value of the estimation error measured by $\|x(k) - \hat{x}(k)\|_2$ and the average relative error measured by $\|x(k) - \hat{x}(k)\|_2/\|x(k)\|_2$. At each time instant, the values are computed over 50 Monte Carlo simulations. As shown in Fig. 3, the average estimation error remains comparable across different noise distributions, while the average relative error exhibits a rapid initial decay and subsequently stabilizes at a low level, thereby demonstrating robustness of the proposed method against the measurement noises.

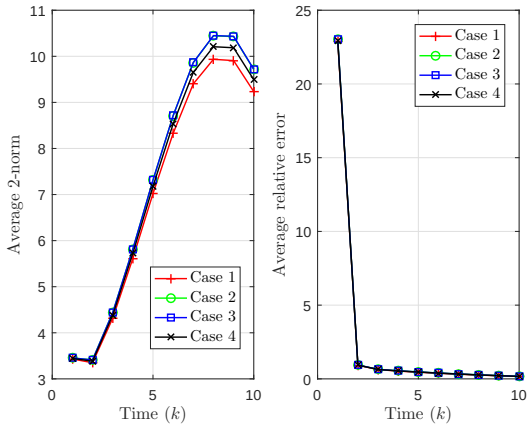

Fig. 3: The average 2-norm of the estimation errors (Left) and the average relative error (Right) in different four cases, which are computed over 50 Monte Carlo runs.

Example 2: Consider the following damped nonlinear pendulum equation

$$\dot{\theta} = \omega + w^{(1)}, \quad \dot{\omega} = -\mu\omega - \frac{g}{L}\sin\theta + w^{(2)}.$$

Here, with a slight abuse of notation, θ and ω are used again to represent the angular displacement and the angular velocity of the pendulum, respectively; g is the gravitational acceleration, L is the length of the pendulum, μ is the damping coefficient, $w^{(1)}$ and $w^{(2)}$ describe the external disturbances.

Applying the Euler discretization method to the pendulum equation, we have

$$\theta(k+1) = \theta(k) + T\omega(k) + Tw^{(1)}(k)$$

$$\omega(k+1) = \omega(k) - T\mu\omega(k) - T\frac{g}{L}\sin\theta(k) + Tw^{(2)}(k).$$

The measurements of the pendulum are given as follows:

$$y_1(k) = \theta(k) + v_1(k), \quad y_2(k) = \omega(k) + v_2(k).$$

In this example, the sampling period is chosen as $T = 0.01\,\mathrm{s}$, and parameters of the pendulum are set as $g = 9.8\,\mathrm{m/s^2}$, $L = 1\,\mathrm{m}$, and $\mu = 0.1$. The terms $Tw^{(1)}(k)$, $Tw^{(2)}(k)$, $v_1(k)$ and $v_2(k)$ are drawn from uniform distributions on $[-0.01, 0.01]$, $[-0.1, 0.1]$, $[-0.1, 0.1]$, and $[-0.2, 0.2]$, respectively. The initial state is set to be $(\theta(0), \omega(0)) = (0.1, 0)$. To guarantee that Assumption 1 is satisfied, we set $\mathbf{W} = 0.1I$, $\mathbf{V}_1 = 0.1$, $\mathbf{V}_2 = 0.2$, and $\vec{\mathbf{X}}(0) = 0.1I$. The encoders' parameters are chosen as $\varsigma_1 = \varsigma_2 = 0.1, \tau_1 = \tau_2 = 0.05$. The system state is taken as $x(k) = [\theta(k) \;\; \omega(k)]^T$.

Fig. 4 shows the evolution of the F-radii of the zonotopes computed by Algorithm 1 for values of ν ranging from 0 to 2, as well as the F-radius $\|\hat{\mathcal{E}}_1(k)\|_F$ computed by Theorem 3 with $\nu = 2$. Additional information on the average F-radius is given in TABLE III. These results not only demonstrate effectiveness of Theorem 3 but also support the discussions regarding the selection of ν.

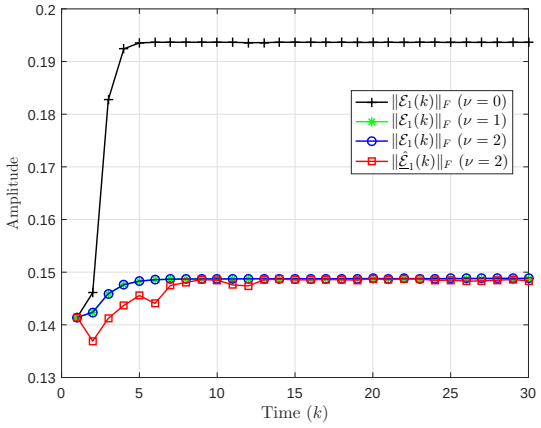

Fig. 4: F-radius under different ν.

TABLE III: Comparison of the average F-radius.

$(1/30)\sum_{k=1}^{30}\|\mathcal{E}_1(k)\|_F \quad (\nu = 0)$	0.1899
$(1/30)\sum_{k=1}^{30}\|\mathcal{E}_1(k)\|_F \quad (\nu = 1)$	0.1481
$(1/30)\sum_{k=1}^{30}\|\mathcal{E}_1(k)\|_F \quad (\nu = 2)$	0.1482
$(1/30)\sum_{k=1}^{30}\|\hat{\mathcal{E}}_1(k)\|_F \quad (\nu = 2)$	0.1471

VI. Conclusion

This paper has studied the zonotopic SME problem for a class of nonlinear systems under an encoding-decoding scheme. To this end, a zonotope-based WMF method was developed, where the decoding signals were fused into a signal with reduced dimensionality. By employing the Carleman approximation, the studied ν+1 times continuously differentiable nonlinear system was transformed into a linear time-varying one with a new expression of the approximation error. A Kalman-type estimator was then constructed, and zonotopes

enclosing the prediction and estimation errors were recursively calculated, and the estimator parameter was designed to minimize the F-radius of the zonotope enclosing the estimation error. The impact of the system smoothness level ν on the estimation performance was analyzed, revealing that higher ν enables more state constraints via estimated Kronecker powers, which can be exploited to further improve accuracy. Moreover, the proposed WMF method achieves estimation accuracy comparable to the parallel fusion method under the polynomial SME framework. Finally, two simulation studies have verified the effectiveness of the proposed approach.

APPENDIX A

Lemma 4: Consider a vector $\omega \in \langle 0, \Omega\rangle \subset \mathbb{R}^n$, where $\Omega = \mathrm{diag}\{\omega^{(1)}, \omega^{(2)}, \ldots, \omega^{(n)}\}$ is a positive definite diagonal matrix with $\omega^{(1)}, \omega^{(2)}, \ldots, \omega^{(n)}$ being scalars. Then, for a given positive integer l, the Kronecker power $\omega^{[l]} \in \mathbb{R}^{n^l}$ satisfies

$$\omega^{[l]} \in \langle \boldsymbol{\omega}(l), \boldsymbol{\Omega}(l)\rangle \tag{63}$$

where $\boldsymbol{\omega}(l)$ and $\boldsymbol{\Omega}(l)$ are calculated as follows:

1) If l is an odd number, then $\boldsymbol{\omega}(l) = 0$ and $\boldsymbol{\Omega}(l) = \Omega^{[l]}$.
2) If l is an even number, then $\boldsymbol{\omega}(l) = \mathrm{vec}_{n^l}\left\{\boldsymbol{\omega}^{(\Im)}(l)\right\}$ is a nonzero vector and $\boldsymbol{\Omega}(l) = \mathrm{diag}_{n^l}\left\{\boldsymbol{\Omega}^{(\Im)}(l)\right\}$ is a diagonal matrix. Here, for an integer $\Im \in \{1, 2, \ldots, n^l\}$, the way to calculate $\boldsymbol{\omega}^{(\Im)}(l)$ and $\boldsymbol{\Omega}^{(\Im)}(l)$ is given as follows: letting positive integers $\wp^{(\Im)}(1), \wp^{(\Im)}(2), \ldots, \wp^{(\Im)}(l)$ be given by

$$\begin{cases} \wp^{(\Im)}(1) = \left\lfloor \dfrac{\Im - 1}{n^{l-1}} \right\rfloor + 1 \\ j^{(\Im)}(1) = \mathrm{mod}(\Im - 1, n^{l-1}) + 1 \\ \wp^{(\Im)}(\hbar) = \left\lfloor \dfrac{j^{(\Im)}(\hbar - 1) - 1}{n^{l-\hbar}} \right\rfloor + 1 \\ j^{(\Im)}(\hbar) = \mathrm{mod}(j^{(\Im)}(\hbar - 1) - 1, n^{l-\hbar}) + 1 \\ \qquad\qquad\qquad\qquad \hbar = 2, 3, \ldots, l-1 \\ \wp^{(\Im)}(l) = j^{(\Im)}(l-1) \end{cases} \tag{64}$$

where, for real numbers φ and ϕ, $\lfloor\varphi\rfloor$ denotes the integral part of φ, and $\mathrm{mod}(\varphi, \phi)$ denotes the remainder of the division of φ by ϕ, respectively; and letting $N^{(\Im)}(i)$ be the number of integers equal to i ($i \in \{1, 2, \ldots, n\}$) among $\wp^{(\Im)}(1), \wp^{(\Im)}(2), \ldots, \wp^{(\Im)}(l)$, if

$$\sum_{i=1}^{n} \mathrm{mod}(N^{(\Im)}(i), 2) > 0 \tag{65}$$

then $\boldsymbol{\omega}^{(\Im)}(l) = 0$ and $\boldsymbol{\Omega}^{(\Im)}(l) = \prod_{i=1}^{n}(\omega^{(i)})^{N^{(\Im)}(i)}$; otherwise, $\boldsymbol{\omega}^{(\Im)}(l) = \frac{1}{2}\prod_{i=1}^{n}(\omega^{(i)})^{N^{(\Im)}(i)}$ and $\boldsymbol{\Omega}^{(\Im)}(l) = \frac{1}{2}\prod_{i=1}^{n}(\omega^{(i)})^{N^{(\Im)}(i)}$.

Proof: Due to $\omega \in \langle 0, \Omega\rangle$, according to Definition 1, there must exist a vector $z = [z^{(1)}\ z^{(2)}\ \cdots\ z^{(n)}]^T$ with $\|z\|_\infty \le 1$ such that $\omega = \Omega z = \mathrm{vec}_n\{\omega^{(i)} z^{(i)}\}$, which implies that $\omega^{[l]} = \Omega^{[l]} z^{[l]}$. Noticing that $\|z^{[l]}\|_\infty \le 1$, one can easily obtain from Definition 1 that $\omega^{[l]} \in \langle 0, \Omega^{[l]}\rangle$ holds for each positive integer l. Therefore, when l is an odd number, one has that $\boldsymbol{\omega}(l) = 0$ and $\boldsymbol{\Omega}(l) = \Omega^{[l]}$.

For the case that l is an even number, it is not difficult to deduce from (2.2.3) of [10] that, when $\wp^{(\Im)}(1), \wp^{(\Im)}(2), \ldots, \wp^{(\Im)}(l)$ are calculated by (64), the $\Im$-th component of vector $\omega^{[l]}$ equals $\prod_{i=1}^{n}\left(\omega^{(i)} z^{(i)}\right)^{N^{(\Im)}(i)}$.

When (65) holds, it is obvious that there has one or more odd numbers among $N^{(\Im)}(1), N^{(\Im)}(2), \ldots, N^{(\Im)}(n)$. Recalling that the $\Im$-th component of the vector $\omega^{[l]}$ equals $\prod_{i=1}^{n}\left(\omega^{(i)} z^{(i)}\right)^{N^{(\Im)}(i)}$, one can obtain that the $\Im$-th component of the vector $\omega^{[l]}$ belongs to the interval $[-\prod_{i=1}^{n}(\omega^{(i)})^{N^{(\Im)}(i)}, \prod_{i=1}^{n}(\omega^{(i)})^{N^{(\Im)}(i)}]$. In the same way, one can obtain that, when (65) is not satisfied (i.e., $N^{(\Im)}(1), N^{(\Im)}(2), \ldots, N^{(\Im)}(n)$ are all even numbers), the $\Im$-th component of the vector $\omega^{[l]}$ belongs to the interval $[0, \prod_{i=1}^{n}(\omega^{(i)})^{N^{(\Im)}(i)}]$. Based on the above analysis, it is easy to see from Definition 1 that (63) holds. The proof is now complete. ∎

APPENDIX B

Lemma 5: For matrices $Y = (y_{\underline{i}\underline{j}})_{m_1\times n_1}$ and $Z = (z_{\bar{i}\bar{j}})_{m_2\times n_2}$, one has $\|Y \otimes Z\|_\infty = \|Y\|_\infty \cdot \|Z\|_\infty$.

Proof: In light of the definition of the matrix infinity norm, it follows that

$$\begin{aligned} &\|Y \otimes Z\|_\infty \\ &= \max_{\underline{i}\in\{1,2,\ldots,m_1\}} \left\| \begin{bmatrix} y_{\underline{i}1}Z & \cdots & y_{\underline{i}n_1}Z \end{bmatrix} \right\|_\infty \\ &= \max_{\underline{i}\in\{1,2,\ldots,m_1\}} \max_{\bar{i}\in\{1,2,\ldots,m_2\}} \sum_{\underline{j}=1}^{n_1} |y_{\underline{i}\underline{j}}| \cdot \sum_{\bar{j}=1}^{n_2} |z_{\bar{i}\bar{j}}| \\ &= \Big(\max_{\underline{i}\in\{1,2,\ldots,m_1\}} \sum_{\underline{j}=1}^{n_1} |y_{\underline{i}\underline{j}}|\Big)\Big(\max_{\bar{i}\in\{1,2,\ldots,m_2\}} \sum_{\bar{j}=1}^{n_2} |z_{\bar{i}\bar{j}}|\Big) \\ &= \|Y\|_\infty \cdot \|Z\|_\infty \end{aligned}$$

which ends the proof. ∎

APPENDIX C

Proof of Theorem 1: For presentation clarity, we divide the proof into the following steps.

Step 1 Let us first prove that

$$\tilde{w}(k) \in \left\langle 0_{\bar{n}\times 1}, \tilde{\mathbf{W}}(k)\right\rangle. \tag{66}$$

According to (20), it follows from Lemma 5 that

$$\begin{aligned} &\|\tilde{w}(l,k)\|_\infty \\ &\le \sum_{h=0}^{\nu}\sum_{p=0}^{l} \frac{1}{h!}\|M(l,p,n)\|_\infty \cdot \left\|w^{[l-p]} - \mathbf{w}(l-p)\right\|_\infty \\ &\quad \cdot \left\| \left(\nabla_x^{[h]} \otimes f^{[p]}\right)\Big|_{x(k)=\hat{x}(k)} \right\|_\infty \cdot \left\|x(k) - \hat{x}(k)\right\|_\infty^h. \end{aligned} \tag{67}$$

With (32), it is easy to see that there exists a vector $\varrho(k) \in \mathbb{R}^{\bar{n}}$ satisfying $\|\varrho(k)\|_\infty \le 1$ such that

$$x(k) - \hat{x}(k) = \mathcal{E}_1(k)\varrho(k) \tag{68}$$

which further implies

$$\|x(k) - \hat{x}(k)\|_\infty^h = \|\mathcal{E}_1(k)\varrho(k)\|_\infty^h \le \|\mathcal{E}_1(k)\|_\infty^h. \tag{69}$$

Similarly, one can obtain from (16) that

$$\big\|w^{[l-p]}-\mathbf{w}(l-p)\big\|_\infty \le \|\mathbf{W}(l-p)\|_\infty. \tag{70}$$

On the basis of (67)–(70), it follows from Lemma 2 that

$$\vec{w}(l,k)\in\langle 0_{n^l\times 1},\tilde{\mathbf{w}}(l,k)I_{n^l}\rangle$$

which, together with Definition 1, gives (66).

Step 2 We now proceed to prove that

$$\vec{\mathscr{O}}(k)\in\langle 0_{\bar{n}\times 1},\tilde{\vec{\mathscr{O}}}(k)\rangle. \tag{71}$$

By using Lemma 3, one obtains

$$\begin{aligned}
&\nabla_x^{[\nu+1]}\otimes\big(\Lambda^{(\Im)}(f+w)^{[l]}\big)\\
&=\nabla_x^{[\nu+1]}\otimes\Big(\Lambda^{(\Im)}\sum_{p=0}^{l}M(l,p,n)\big(f^{[p]}\otimes w^{[l-p]}\big)\Big)\\
&=\Lambda^{(\Im)}\sum_{p=0}^{l}M(l,p,n)\Big(\nabla_x^{[\nu+1]}\otimes\big(f^{[p]}\otimes w^{[l-p]}\big)\Big)\\
&=\Lambda^{(\Im)}\sum_{p=0}^{l}M(l,p,n)\Big(\nabla_x^{[\nu+1]}\otimes\big(f^{[p]}\otimes(\mathbf{w}(l-p)\\
&\quad+w^{[l-p]}-\mathbf{w}(l-p))\big)\Big)\\
&=\aleph_1(k)+\aleph_2(k)
\end{aligned}\tag{72}$$

where

$$\begin{aligned}
\aleph_1(k)&\triangleq\Lambda^{(\Im)}\sum_{p=0}^{l}M(l,p,n)\Big(\nabla_x^{[\nu+1]}\otimes\big(f^{[p]}\otimes\mathbf{w}(l-p)\big)\Big)\\
\aleph_2(k)&\triangleq\Lambda^{(\Im)}\sum_{p=0}^{l}M(l,p,n)\Big(\nabla_x^{[\nu+1]}\otimes\big(f^{[p]}\otimes\big(w^{[l-p]}\\
&\qquad-\mathbf{w}(l-p)\big)\big)\Big).
\end{aligned}$$

Noticing the fact that

$$\begin{aligned}
\Gamma^{(\Im)}\breve{x}(k)&=\theta^{(\Im)}(k)x(k)+(1-\theta^{(\Im)}(k))\hat{x}(k)\\
&=\hat{x}(k)+\theta^{(\Im)}(k)e_1(k)\in\langle\hat{x}(k),\mathcal{E}_1(k)\rangle
\end{aligned}\tag{73}$$

where $e_1(k)\triangleq\mathcal{I}e(k|k)$, it is easy to obtain from Lemma 5 that

$$\begin{aligned}
&\|\aleph_1(k)|_{x(k)=\Gamma^{(\Im)}\breve{x}(k)}\|_\infty\\
&\le\sum_{p=0}^{l}\|\Lambda^{(\Im)}\|_\infty\cdot F(p,k)\cdot\|M(l,p,n)\|_\infty\cdot\|\mathbf{w}(l-p)\|_\infty\\
&=\sum_{p=0}^{l}F(p,k)\cdot\|M(l,p,n)\|_\infty\cdot\|\mathbf{w}(l-p)\|_\infty
\end{aligned}\tag{74}$$

and

$$\begin{aligned}
&\|\aleph_2(k)|_{x(k)=\Gamma^{(\Im)}\breve{x}(k)}\|_\infty\\
&\le\sum_{p=0}^{l}\|\Lambda^{(\Im)}\|_\infty\cdot F(p,k)\cdot\|M(l,p,n)\|_\infty\cdot\|\mathbf{W}(l-p)\|_\infty\\
&=\sum_{p=0}^{l}F(p,k)\cdot\|M(l,p,n)\|_\infty\cdot\|\mathbf{W}(l-p)\|_\infty.
\end{aligned}\tag{75}$$

In view of (72)–(75), one has

$$\begin{aligned}
&\Big\|\Big(\nabla_x^{[\nu+1]}\otimes\big(\Lambda^{(\Im)}(f+w)^{[l]}\big)\Big)\Big|_{x(k)=\Gamma^{(\Im)}\breve{x}(k)}\Big\|_\infty\\
&\le\|\aleph_1(k)|_{x(k)=\Gamma^{(\Im)}\breve{x}(k)}\|_\infty+\|\aleph_2(k)|_{x(k)=\Gamma^{(\Im)}\breve{x}(k)}\|_\infty\\
&=\sum_{p=0}^{l}\|\Lambda^{(\Im)}\|_\infty\cdot F(p)\cdot\|M(l,p,n)\|_\infty\cdot\big(\|\mathbf{w}(l-p)\|_\infty\\
&\qquad+\|\mathbf{W}(l-p)\|_\infty\big).
\end{aligned}\tag{76}$$

Recalling (68) and the definitions of $\mathscr{R}(l,\breve{x}(k),w(k))$ and $\vec{\mathscr{O}}(l,k)$ (as shown under (17)), one can derive from (76) and Lemma 5 that the $\Im$-th component of vector $\vec{\mathscr{O}}(l,k)$ (denoted as $\vec{\mathscr{O}}^{(\Im)}(l,k)$) satisfies

$$\begin{aligned}
&\|\vec{\mathscr{O}}^{(\Im)}(l,k)\|_\infty\\
&=\|\mathscr{R}^{(\Im)}(l,\breve{x}(k),w(k))(x(k)-\hat{x}(k))^{[\nu+1]}\|_\infty\\
&\le\|\mathscr{R}^{(\Im)}(l,\breve{x}(k),w(k))\|_\infty\cdot\|(x(k)-\hat{x}(k))^{[\nu+1]}\|_\infty\\
&\le\ \tilde{o}(l,k)
\end{aligned}\tag{77}$$

where $\mathscr{R}^{(\Im)}(l,\breve{x}(k),w(k))$ is the $\Im$-row of matrix $\mathscr{R}(l,\breve{x}(k),w(k))$. Then, applying Lemma 2 to (77) leads to $\vec{\mathscr{O}}^{(\Im)}(l,k)\in\langle 0,\tilde{o}(l,k)\rangle$, which together with Definition 1 gives

$$\vec{\mathscr{O}}(l,k)\in\langle 0_{n^l\times 1},\overleftarrow{\mathscr{O}}(l,k)\rangle. \tag{78}$$

Using Definition 1 again, one can easily obtain from (78) that (71) is true.

Step 3 We now prove (33). With (32), (66) and (71), applying Lemma 1 to (29) yields

$$\begin{aligned}
e(k+1|k)\in&\big(\mathscr{A}(k)\odot\langle 0_{\bar{n}\times 1},\mathcal{E}(k)\rangle\big)\oplus\big\langle 0_{\bar{n}\times 1},\tilde{\mathbf{W}}(k)\big\rangle\\
&\oplus\langle 0_{\bar{n}\times 1},\tilde{\vec{\mathscr{O}}}(k)\rangle\\
=&\langle 0_{\bar{n}\times 1},\underline{\mathcal{E}}(k+1)\rangle
\end{aligned}$$

which is exactly the result of (33).

Step 4 We continue to prove (34). It has been proven that (14) and (33) hold. Then, applying Lemma 1 to (30) results in

$$\begin{aligned}
&e(k+1|k+1)\\
&\in\Big(\big(I-\mathcal{K}(k+1)\tilde{\mathcal{M}}(k+1)\big)\odot\langle 0_{\bar{n}\times 1},\underline{\mathcal{E}}(k+1)\rangle\Big)\\
&\quad\oplus\big((-\mathcal{K}(k+1))\odot\big\langle 0,\tilde{\mathbf{V}}(k+1)\big\rangle\big)\\
&=\langle 0_{\bar{n}\times 1},\mathcal{E}(k+1)\rangle.
\end{aligned}$$

The proof is now complete.

APPENDIX D

Proof of Theorem 2: According to the definition of $\mathscr{I}$, matrix $\mathcal{K}(k+1)$ can be expressed as $\mathcal{K}(k+1)=\mathscr{I}K(k+1)$. Then, it follows from Definition 2 that

$$\begin{aligned}
&\|\mathcal{E}(k+1)\|_F^2\\
&=\mathrm{Tr}\Big\{\big\|K^T(k+1)\mathscr{I}^T-\Phi^{-1}(k+1)\acute{\mathcal{M}}(k+1)\\
&\quad\cdot\underline{\mathcal{P}}(k+1)\big\|^2_{\Phi(k+1)}-\underline{\mathcal{P}}(k+1)\acute{\mathcal{M}}^T(k+1)\Phi^{-1}(k+1)\\
&\quad\cdot\acute{\mathcal{M}}(k+1)\underline{\mathcal{P}}(k+1)+\underline{\mathcal{P}}(k+1)\Big\}
\end{aligned}\tag{79}$$

which implies that, when

$$K^T(k+1)\acute{\mathscr{I}}^T - \Phi^{-1}(k+1)\acute{\mathcal{M}}(k+1)\underline{\mathcal{P}}(k+1) = 0$$

the F-radius of the zonotope in (34) is minimized. Noticing $\acute{\mathscr{I}}^T\acute{\mathscr{I}} = I_{\bar{n}-1}$, it is easy to see that the estimator parameter given in (42) can minimize the F-radius of the zonotope in (34).

APPENDIX E

Proof of Proposition 2: From (79), one can see that with the estimator parameter $K(k)$ designed by (42), the following equality holds:

$$\mathcal{E}(k)\mathcal{E}^T(k) = \underline{\mathcal{P}}(k) - \underline{\mathcal{P}}(k)\acute{\mathcal{M}}^T(k)\Phi^{-1}(k)\acute{\mathcal{M}}(k)\underline{\mathcal{P}}(k)$$

which means that

$$\begin{aligned}\mathcal{I}\mathcal{E}(k)\mathcal{E}^T(k)\mathcal{I}^T \geq& \mathcal{I}(\underline{\mathcal{P}}(k) - \underline{\mathcal{P}}(k)\acute{\mathcal{M}}^T(k)\Phi^{-1}(k)\\ &\cdot \acute{\mathcal{M}}(k)\underline{\mathcal{P}}(k))\mathcal{I}^T\end{aligned}$$

holds for any $K(k)$.

With the above inequality, it can be deduced that the F-radius of the zonotope in (43) satisfies

$$\begin{aligned}\|\mathcal{I}\mathcal{E}(k)\|_F^2 \geq& \mathrm{Tr}\{\mathcal{I}(\underline{\mathcal{P}}(k) - \underline{\mathcal{P}}(k)\acute{\mathcal{M}}^T(k)\Phi^{-1}(k)\\ &\cdot \acute{\mathcal{M}}(k)\underline{\mathcal{P}}(k))\mathcal{I}^T\}\end{aligned}$$

which, together with $\mathcal{E}_1(k) = \mathcal{I}\mathcal{E}(k)$, implies that the estimator parameter $K(k)$ in (42) is a solution to the optimization problem $\min_{K(k)} \|\mathcal{E}_1(k)\|_F$. The proof is now complete.

APPENDIX F

Proof of Theorem 3: We first prove (49). According to (37) and (43), one has

$$(I - L(k)\Xi_1(k))\mathcal{I}e(k|k) \in \langle 0, (I - L(k)\Xi_1(k))\mathcal{E}_1(k)\rangle. \tag{80}$$

Additionally, similar to (77), it can be obtained that

$$-L(k)\sum_{h=2}^{\nu}\Xi_h(k)(x(k) - \hat{x}(k))^{[h]} \in \langle 0, -\kappa(k)L(k)\rangle. \tag{81}$$

Furthermore, recalling $\|\eta(k)\|_\infty \leq 1$, one can see that

$$L(k)\mathcal{E}^{[2:\nu]}(k)\eta(k) \in \langle 0, L(k)\mathcal{E}^{[2:\nu]}(k)\rangle. \tag{82}$$

Combining (80)–(82) and applying Lemma 1 to (48), the formula (49) follows directly.

Derivations of the optimal estimator gain and the associated $\|\hat{\underline{\mathcal{E}}}_1(k)\|_F$ follow analogous steps to those presented in the proof of Theorem 2, and therefore are omitted for brevity.

APPENDIX G

Proof of Theorem 4: To prove this theorem, we first prove

$$\mathcal{P}(k+1) = \mathcal{P}^{\mathrm{PF}}(k+1) \tag{83}$$

where $\mathcal{P}^{\mathrm{PF}}(k+1) \triangleq \mathcal{E}^{\mathrm{PF}}(k+1)(\mathcal{E}^{\mathrm{PF}}(k+1))^T$ and $\mathcal{P}(k+1) \triangleq \mathcal{E}(k+1)\mathcal{E}^T(k+1)$.

From the proof of Theorem 2, it can be seen that, with the estimator parameter $K(k+1)$ designed in (42), the following holds:

$$\begin{aligned}\mathcal{P}(k+1) =& \underline{\mathcal{P}}(k+1) - \underline{\mathcal{P}}(k+1)\acute{\mathcal{M}}^T(k+1)\Phi^{-1}(k+1)\\ &\cdot \acute{\mathcal{M}}(k+1)\underline{\mathcal{P}}(k+1)\\ =& \big(\underline{\mathcal{P}}^{-1}(k+1) + \acute{\mathcal{M}}^T(k+1)\\ &\cdot (\acute{\mathbf{V}}(k+1)\acute{\mathbf{V}}^T(k+1))^{-1}\acute{\mathcal{M}}(k+1)\big)^{-1}.\end{aligned} \tag{84}$$

Similarly, one has

$$\begin{aligned}\mathcal{P}^{\mathrm{PF}}(k+1) =& \big(\mathcal{I}^T C^T(k+1)(\breve{\mathbf{V}}\breve{\mathbf{V}}^T)^{-1}C(k+1)\mathcal{I}\\ &+ (\underline{\mathcal{P}}^{\mathrm{PF}}(k+1))^{-1}\big)^{-1}.\end{aligned} \tag{85}$$

According to (33), (56) and (60), one obtains

$$\underline{\mathcal{E}}(k+1) = \underline{\mathcal{E}}^{\mathrm{PF}}(k+1) \tag{86}$$

which leads to

$$\underline{\mathcal{P}}(k+1) = \underline{\mathcal{P}}^{\mathrm{PF}}(k+1). \tag{87}$$

In light of (14) and (15), the following equality

$$\begin{aligned}\acute{\mathbf{V}}(k)\acute{\mathbf{V}}^T(k) =& \big(H^T(k)\mathcal{Q}(k)H(k)\big)^{-1}H^T(k)\mathcal{Q}(k)\breve{\mathbf{V}}\breve{\mathbf{V}}^T\\ &\cdot \mathcal{Q}^T(k)H(k)\big(H^T(k)\mathcal{Q}(k)H(k)\big)^{-1}\\ =& \big(H^T(k)(\breve{\mathbf{V}}\breve{\mathbf{V}}^T)^{-1}H(k)\big)^{-1}\end{aligned} \tag{88}$$

holds for all $k \geq 1$.

By observing (9), (83), (84), (85), (87), (88) and $\acute{\mathcal{M}}(k) = \mathcal{M}(k)\mathcal{I}$, (83) can be immediately obtained.

Having proven (83), we proceed to show (61). Using (25), (53) and (59), we obtain the following:

$$\widehat{x}(k+1|k) = \widehat{x}^{\mathrm{PF}}(k+1|k) \tag{89}$$

which gives rise to

$$e(k+1|k) = e^{\mathrm{PF}}(k+1|k). \tag{90}$$

Notice that the parameters $\mathcal{K}(k+1)$ in (26) and $\mathcal{K}^{\mathrm{PF}}(k+1)$ in (55) can be rewritten as

$$\begin{aligned}\mathcal{K}(k+1) =& \acute{\mathscr{I}}\acute{\mathscr{I}}^T\mathcal{P}(k+1)\acute{\mathcal{M}}^T(k+1)\\ &\cdot \big(\acute{\mathbf{V}}(k+1)\acute{\mathbf{V}}^T(k+1)\big)^{-1}\end{aligned}$$

and

$$\mathcal{K}^{\mathrm{PF}}(k+1) = \acute{\mathscr{I}}\acute{\mathscr{I}}^T\mathcal{P}^{\mathrm{PF}}(k+1)\mathcal{I}^T C^T(k+1)(\breve{\mathbf{V}}\breve{\mathbf{V}}^T)^{-1}$$

respectively, which, together with (9), (83), (88) and $\acute{\mathcal{M}}(k) = \mathcal{M}(k)\mathcal{I}$, gives

$$\mathcal{K}(k+1)\acute{\mathcal{M}}(k+1) = \mathcal{K}^{\mathrm{PF}}(k+1)C(k+1)\mathcal{I}. \tag{91}$$

Furthermore, one can see from (9), (12), (83) and (88) that

$$\mathcal{K}(k+1)\acute{v}(k+1) = \mathcal{K}^{\mathrm{PF}}(k+1)\breve{v}(k+1). \tag{92}$$

With (89), (90), (91) and (92), it can be seen from (24) and (52) that

$$\begin{aligned}&\mathcal{K}(k+1)(\acute{y}(k+1)-\acute{\mathcal{M}}(k+1)\widehat{x}(k+1|k))\\&=\mathcal{K}(k+1)(\acute{\mathcal{M}}(k+1)e(k+1|k)+\acute{v}(k+1))\\&=\mathcal{K}^{\mathrm{PF}}(k+1)(C(k+1)\mathcal{I}e^{\mathrm{PF}}(k+1|k)+\breve{v}(k+1))\\&=\mathcal{K}^{\mathrm{PF}}(k+1)(\breve{y}(k+1)-C(k+1)\mathcal{I}\widehat{x}^{\mathrm{PF}}(k+1|k))\end{aligned}$$

which means that $\widehat{x}(k+1|k+1)$ in (26) and $\widehat{x}^{\mathrm{PF}}(k+1|k+1)$ in (54) satisfy (61).

It remains to show (62). Utilizing (86) and (91) again, one has

$$\begin{aligned}&(I-\mathcal{K}(k+1)\acute{\mathcal{M}}(k+1))\underline{\mathcal{E}}(k+1)\\&=(I-\mathcal{K}^{\mathrm{PF}}(k+1)C(k+1)\mathcal{I})\underline{\mathcal{E}}^{\mathrm{PF}}(k+1).\end{aligned}\tag{93}$$

Moreover, using a similar method in the deduction of (92), one can obtain from (14) that

$$\mathcal{K}(k+1)\acute{\mathbf{V}}(k+1)=\mathcal{K}^{\mathrm{PF}}(k+1)\breve{\mathbf{V}}.\tag{94}$$

Observing (34), (57), (93) and (94), the result of (62) is obvious. The proof is now complete.

REFERENCES

[1] T. Alamo, J. M. Bravo, and E. F. Camacho, "Guaranteed state estimation by zonotopes," *Automatica*, vol. 41, no. 6, pp. 1035–1043, 2005.

[2] L. J. S. Allen and V. L. Kocic, "Resonance in Beverton-Holt population models with periodic and random coefficients," *J. Differ. Equ. Appl.*, vol. 20, nos. 5–6, pp. 925–946, 2014.

[3] J. Bai, Z. Yang, Z. Li, C. Shen, Y. Chen, and J. Li, "Trajectory tracking controller design for wheeled mobile robot with velocity and torque constraints," *Int. J. Syst. Sci.*, vol. 55, no. 14, pp. 2825–2873, 2024.

[4] X. Bai, G. Li, M. Ding, L. Yu and Y. Sun, "Recursive strong tracking filtering for power harmonic detection with outliers-resistant event-triggered mechanism," *Int. J. Netw. Dyn. Intell.*, vol. 3, no. 4, art. no. 100023, 2024.

[5] R. Bellman, *Introduction to Matrix Analysis*. New York, NY, USA: McGraw-Hill, Book Co., Inc., 1960.

[6] D. Bhattacharjee and K. Subbarao, "Set-membership filter for discrete-time nonlinear systems using state-dependent coefficient parameterization," *IEEE Trans. Autom. Control*, vol. 67, no. 2, pp. 894–901, Feb. 2022.

[7] R. Caballero-Águila, A. Hermoso-Carazo, and J. Linares-Pérez, "Distributed fusion filters from uncertain measured outputs in sensor networks with random packet losses," *Inf. Fusion*, vol. 34, pp. 70–79, 2017.

[8] R. Caballero-Águila and J. Linares-Pérez, "Centralized fusion estimation in networked systems: Addressing deception attacks and packet dropouts with a zero-order hold approach," *Int. J. Netw. Dyn. Intell.*, vol. 3, no. 4, art. no. 100021, 2024.

[9] G. Calafiore, "Reliable localization using set-valued nonlinear filters," *IEEE Trans. Syst., Man, Cybern. Part A, Syst. Humans*, vol. 35, no. 2, pp. 189–197, Mar. 2005.

[10] F. Carravetta, A. Germani and M. Raimondi, "Polynomial filtering for linear discrete time non-Gaussian systems," *SIAM J. Control Optim.*, vol. 34, no. 5, pp. 1666–1690, 1996.

[11] B. Chen and G. Hu, "Nonlinear state estimation under bounded noises," *Automatica*, vol. 98, pp. 159–168, 2018.

[12] D. Ciuonzo, A. Aubry, and V. Carotenuto, "Rician MIMO channel- and jamming-aware decision fusion," *IEEE Trans. Signal Process.*, vol. 65, no. 15, pp. 3866–3880, Aug. 2017.

[13] D. Ciuonzo, V. Carotenuto, and A. De Maio, "On multiple covariance equality testing with application to SAR change detection," *IEEE Trans. Signal Process.*, vol. 65, no. 19, pp. 5078–5091, Oct. 2017.

[14] C. Combastel, "Zonotopes and Kalman observers: Gain optimality under distinct uncertainty paradigms and robust convergence," *Automatica*, vol. 55, pp. 265–273, 2015.

[15] D. Dai, J. Li, Y. Song, and F. Yang, "Event-based recursive filtering for nonlinear bias-corrupted systems with amplify-and-forward relays," *Syst. Sci. Control Eng.*, vol. 12, no. 1, art. no. 2332419, 2024.

[16] A. A. de Paula, D. M. Raimondo, G. V. Raffo, and B. O. S. Teixeira, "Set-based state estimation for discrete-time constrained nonlinear systems: An approach based on constrained zonotopes and DC programming," *Automatica*, vol. 159, art. no. 111401, 2024.

[17] Z. Fei, L. Yang, X.-M. Sun, and S. Ren, "Zonotopic set-membership state estimation for switched systems with restricted switching," *IEEE Trans. Autom. Control*, vol. 67, no. 11, pp. 6127-6134, Nov. 2022.

[18] P. Gao, C. Jia, and A. Zhou, "Encryption-decryption-based state estimation for nonlinear complex networks subject to coupled perturbation," *Syst. Sci. Control Eng.*, vol. 12, no. 1, art. no. 2357796, 2024.

[19] X. Ge, Q.-L. Han, and F. Yang, "Event-based set-membership leader-following consensus of networked multi-agent systems subject to limited communication resources and unknown-but-bounded noise," *IEEE Trans. Ind. Electron.*, vol. 64, no. 6, pp. 5045–5054, Jun. 2017.

[20] A. Germani, C. Manes, and P. Palumbo, "Polynomial extended Kalman filtering for discrete-time nonlinear stochastic systems," In: *Proc. 42nd IEEE Conf. Decis. Control*, Maui, Hawaii USA, pp. 886–891, Dec. 2003.

[21] S. T. Goh, O. Abdelkhalik, and S. A. R. Zekavat, "A weighted measurement fusion Kalman filter implementation for UAV navigation," *Aerosp. Sci. Technol.*, vol. 28, no. 1, pp. 315–323, 2013.

[22] G. Hao and S.-L. Sun, "Distributed fusion cubature Kalman filters for nonlinear systems," *Int. J. Robust Nonlinear Control*, vol. 29, no. 17, pp. 5979–5991, 2019.

[23] G. Hao, S.-L. Sun, and Y. Li, "Nonlinear weighted measurement fusion unscented Kalman filter with asymptotic optimality," *Inf. Sci.*, vol. 299, pp. 85–98, 2015.

[24] W. Kühn, "Rigorously computed orbits of dynamical systems without the wrapping effect," *Computing*, vol. 61, pp. 47–67, 1998.

[25] C. L. Lawson and R. J. Hanson, *Solving Least Squares Problems*. Philadelphia, USA: SIAM, 1995.

[26] V. T. H. Le, C. Stoica, T. Alamo, E. F. Camacho, and D. Dumur, *Zonotopes: From Guaranteed State-Estimation to Control*, ISTE Ltd, 2013.

[27] C. Li, Y. Liu, M. Gao, and L. Sheng, "Fault-tolerant formation consensus control for time-varying multi-agent systems with stochastic communication protocol," *Int. J. Netw. Dyn. Intell.*, vol. 3, no. 1, art. no. 100004, 2024.

[28] J. Li, H. Dong, Y. Shen, and N. Hou, "Encoding-decoding strategy based resilient state estimation for bias-corrupted stochastic nonlinear systems," *ISA Trans.*, vol. 127, pp. 80–87, 2022.

[29] T. Li and L. Xie, "Distributed coordination of multi-agent systems with quantized-observer based encoding-decoding," *IEEE Trans. Autom. Control*, vol. 57, no. 12, pp. 3023–3037, Dec. 2012.

[30] X. R. Li, Y. Zhu, J. Wang, and C. Han, "Optimal linear estimation fusion-Part I: Unified fusion rules," *IEEE Trans. Inf. Theory*, vol. 49, no. 9, pp. 2192–2208, Sep. 2003.

[31] H. Lin and S. Sun, "Optimal sequential estimation for asynchronous sampling discrete-time systems," *IEEE Trans. Signal Process.*, vol. 68, pp. 6117–6127, Oct. 2020.

[32] L. Liu, L. Ma, J. Guo, J. Zhang, and Y. Bo, "Distributed set-membership filtering for time-varying systems: A coding-decoding-based approach," *Automatica*, vol. 129, art. no. 109684, 2021.

[33] L.-N. Liu and G.-H. Yang, "Distributed energy resource coordination for a microgrid over unreliable communication network with DoS attacks," *Int. J. Syst. Sci.*, vol. 55, no. 2, pp. 237–252, 2024.

[34] Q. Liu and Z. Wang, "Moving-horizon estimation for linear dynamic networks with binary encoding schemes," *IEEE Trans. Autom. Control*, vol. 66, no. 4, pp. 1763–1770, Apr. 2021.

[35] W.-Q. Liu, X.-M. Wang, and Z.-L. Deng, "Robust centralized and weighted measurement fusion Kalman estimators for uncertain multisensor systems with linearly correlated white noises," *Inf. Fusion*, vol. 35, pp. 11–25, 2017.

[36] Y. Liu, Z. Wang, X. He, and D. Zhou, "Filtering and fault detection for nonlinear systems with polynomial approximation," *Automatica*, vol. 54, pp. 348–359, 2015.

[37] Y. Liu, Z. Wang and D. Zhou, "Quantised polynomial filtering for nonlinear systems with missing measurements," *Int. J. Control*, vol. 91, no. 10, pp. 2250–2260, 2018.

[38] E. Mousavinejad, X. Ge, Q.-L. Han, T. J. Lim, and L. Vlacic, "An ellipsoidal set-membership approach to distributed joint state and sensor fault estimation of autonomous ground vehicles," *IEEE/CAA J. Autom. Sinica*, vol. 8, no. 6, pp. 1107-1118, Jun. 2021.

[39] L. Orihuela, "Comparison of the guaranteed state estimator and the zonotopic Kalman filter for linear time-variant systems," *IEEE Control Syst. Lett.*, vol. 7, pp. 1512–1517, May 2023.

[40] P. Pillay and R. Krishnan, "Control characteristics and speed controller design for a high performance permanent magnet synchronous motor

drive," *IEEE Trans. Power Electron.*, vol. 5, no. 2, pp. 151–159, Apr. 1990.
[41] X. Qing, F. Yang, and X. Wang, "Extended set-membership filter for power system dynamic state estimation," *Elect. Power Syst. Res.*, vol. 99, pp. 56–63, 2013.
[42] M. R. S. Raj, A. G. M. Selvam, and R. Janagaraj, "Stability in a discrete prey-predator model," *Int. J. Latest Res. Sci. Technol.*, vol. 2, no. 1, pp. 482–485, 2013.
[43] L. Sheng, Y. Wang, M. Gao, Y. Niu, and D. Zhou, "Finite-time H_∞ filtering for nonlinear stochastic systems with multiplicative noises via Carleman linearization technique," *IEEE Trans. Aerosp. Electron. Syst.*, vol. 59, no. 2, pp. 1774–1786, Apr. 2023.
[44] S. Sun, "Distributed optimal linear fusion predictors and filters for systems with random parameter matrices and correlated noises," *IEEE Trans. Signal Process.*, vol. 68, pp. 1064–1074, Jan. 2020.
[45] J. Wan, S. Sharma, and R. Sutton, "Guaranteed state estimation for nonlinear discrete-time systems via indirectly implemented polytopic set computation," *IEEE Trans. Autom. Control*, vol. 63, no. 12, pp. 4317–4322, Dec. 2018.
[46] Y. Wang, V. Puig, and G. Cembrano, "Set-membership approach and Kalman observer based on zonotopes for discrete-time descriptor systems," *Automatica*, vol. 93, pp. 435–443, 2018.
[47] Y. Wang, Z. Wang, V. Puig, and G. Cembrano, "Zonotopic set-membership state estimation for discrete-time descriptor LPV systems," *IEEE Trans. Autom. Control*, vol. 64, no. 5, pp. 2092–2099, May 2019.
[48] Z. Wang, X. Shen, H. Liu, F. Meng, and Y. Zhu, "Dual set membership filter with minimizing nonlinear transformation of ellipsoid," *IEEE Trans. Autom. Control*, vol. 67, no. 5, pp. 2405–2418, May 2022.
[49] H. Yang, H. Yan, Z. Li, M. Wang, and F. Yang, "Set-membership estimation for nonlinear systems based on zonotope analysis," *Automatica*, vol. 177, art. no. 112278, 2025.
[50] J. Yin, F. Yan, Y. Liu, G. He, and Y. Zhuang, "An overview of simultaneous localisation and mapping: Towards multi-sensor fusion," *Int. J. Syst. Sci.*, vol. 55, no. 3, pp. 550–568, 2024.
[51] S. Zhang, L. Ma, and X. Yi, "Model-free adaptive control for nonlinear multi-agent systems with encoding-decoding mechanism," *IEEE Trans. Signal Inf. Process. Netw.*, vol. 8, pp. 489–498, Jun. 2022.
[52] S. Zhang, V. Puig, and S. Ifqir, "Set-membership estimation of switched LPV systems: Application to fault/disturbance estimation," *Int. J. Robust Nonlinear Control*, vol. 37, no. 7, pp. 4509–4531, 2024.
[53] W.-A. Zhang, K. Zhou, X. Yang, and A. Liu, "Sequential fusion estimation for networked multisensor nonlinear systems," *IEEE Trans. Ind. Electron.*, vol. 67, no. 6, pp. 4991–4999, Jun. 2020.
[54] Y. Zhang, N. Xia, Q.-L. Han, and F. Yang, "Set-membership global estimation of networked systems," *IEEE Trans. Cybern.*, vol. 52, no. 3, pp. 1454–1464, Mar. 2022.
[55] P. Zhao, H. Liu, T. Huang, and H. Tan, "Trust-based distributed state estimation for microgrids with encoding-decoding mechanisms," *Inf. Sci.*, vol. 639, art. no. 118946, 2023.
[56] Z. Zhao, Z. Wang, L. Zou, Y. Chen, and W. Sheng, "Zonotopic distributed fusion for nonlinear networked systems with bit rate constraint," *Inf. Fusion*, vol. 90, pp. 174–184, 2023.
[57] Z. Zhao, Z. Wang, L. Zou, H. Liu, and W. Sheng, "Zonotope-based distributed set-membership fusion estimation for artificial neural networks under the dynamic event-triggered mechanism," *IEEE Trans. Neural Netw. Learn. Syst.*, vol. 36, no. 1, pp. 1637–1650, Jan. 2025.
[58] L. Zhou and V. Kumar, "Robust multi-robot active target tracking against sensing and communication attacks," *IEEE Trans. Robot.*, vol. 39, no. 3. pp. 1768–1780, Jun. 2023.
[59] M. Zhou, Y. Wu, J. Wang, T. Xue, and T. Raïssi, Zonotopic state estimation and sensor fault detection for a wastewater treatment bioprocess, *Int. J. Robust Nonlinear Control*, vol. 34, no. 14, pp. 9298–9315, 2024.
[60] M. Zhu, R. Wang, and X.-M. Sun, "The optimal distributed weighted least-squares estimation in finite steps for networked systems," *IEEE Trans. Circuits Syst. II, Exp. Briefs*, vol. 70, no. 3, pp. 1069–1073, Mar. 2023.

Zhongyi Zhao (Member, IEEE) received the B.Eng. degree in electrical engineering and automation in 2016 and the Ph.D. degree in control theory and control engineering in 2023, both from the Shandong University of Science and Technology, Qingdao, China.

He is currently a Postdoctoral Research Fellow with the School of Mathematics, Southeast University, Nanjing, China. From November 2021 to October 2022, he was a visiting Ph.D. student with the Department of Computer Science, Brunel University London, Uxbridge, U.K. His current research interests include networked systems, multi-sensor information fusion, and set-membership estimation.

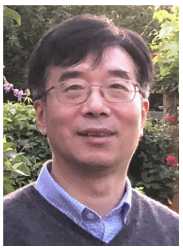

Zidong Wang (SM'03-F'14) received the B.Sc. degree in mathematics in 1986 from Suzhou University, Suzhou, China, and the M.Sc. degree in applied mathematics in 1990 and the Ph.D. degree in electrical engineering in 1994, both from Nanjing University of Science and Technology, Nanjing, China.

He is currently a Professor of Dynamical Systems and Computing in the Department of Computer Science, Brunel University London, U.K. From 1990 to 2002, he held teaching and research appointments in universities in China, Germany and the U.K. Prof. Wang's research interests include dynamical systems, signal processing, bioinformatics, control theory and applications. He has published a number of papers in international journals. He is a holder of the Alexander von Humboldt Research Fellowship of Germany, the JSPS Research Fellowship of Japan, William Mong Visiting Research Fellowship of Hong Kong.

Prof. Wang serves (or has served) as the Editor-in-Chief for *International Journal of Systems Science*, the Editor-in-Chief for *Neurocomputing*, the Editor-in-Chief for *Systems Science & Control Engineering*, and an Associate Editor for 12 international journals including IEEE Transactions on Automatic Control, IEEE Transactions on Control Systems Technology, IEEE Transactions on Neural Networks, IEEE Transactions on Signal Processing, and IEEE Transactions on Systems, Man, and Cybernetics-Part C. He is a Member of the Academia Europaea, a Member of the European Academy of Sciences and Arts, an Academician of the International Academy for Systems and Cybernetic Sciences, a Fellow of the IEEE, a Fellow of the Royal Statistical Society and a member of program committee for many international conferences.

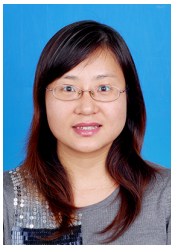

Jinling Liang received the B.Sc. and M.Sc. degrees in mathematics from Northwest University, Xi'an, China, in 1997 and 1999, respectively, and the Ph.D. degree in applied mathematics from Southeast University, Nanjing, China, in 2006.

She is currently a Professor in the School of Mathematics, Southeast University, Nanjing, China. She has published around 90 papers in refereed international journals. Her current research interests include stochastic systems, complex networks, robust filtering and bioinformatics. She serves as an associate editor for several international journals.

Wenying Xu (Senior Member, IEEE) received M.S. degree in Applied Mathematics from Southeast University, Nanjing, China, in 2014, and the Ph.D. degree in applied mathematics from the City University of Hong Kong, Hong Kong, in 2017.

Prof. Xu is currently a Professor in the School of Mathematics, Southeast University, China. Prior to her current position, she was a Post-Doctoral Fellow in Potsdam Institute for Climate Impact Research, Potsdam, Germany from 2019 to 2021, and a Research Fellow in the School of Electrical and Electronic Engineering, Nanyang Technological University, Singapore from 2017 to 2018, respectively. From May 2015 to Aug. 2015 and from Oct. 2019 to Dec. 2019, she severed as an Academic Visitor in the Department of Computer Science, Brunel University London, U.K. Her current research interests include cyber-physical system, game theory in networks, distributed event-triggered control, and distributed cooperative control.

Prof. Xu serves as an Associate Editor for *IEEE Transactions on Systems, Man, and Cybernetics: Systems* and *Systems & Control Letters*; and a Senior Member of *IEEE*. Prof. Xu was a recipient of an Alexander von Humboldt Fellowship in 2018.